Master Thesis in Geographical Information Science nr 94

Spatial-temporal GIS analysis in public health – a case study of polio disease

Roman Spataru

2018
Department of
Physical Geography and Ecosystem Science
Centre for Geographical Information Systems
Lund University
Sölvegatan 12
S-223 62 Lund
Sweden

Roman Spataru (2018). Spatial-temporal GIS analysis in public health - a case study of polio disease

Master degree thesis, 30/ credits in Master in Geographical Information Science

Department of Physical Geography and Ecosystem Science, Lund University

Spatial-temporal GIS analysis in public health – a case study of polio disease

---

Roman Spataru

Master thesis, 30 credits, in Geographical Information Sciences

Supervisor Dr. Ali Mansourian

Lund University GIS Centre, Department of Physical Geography and Ecosystem Science, Lund University

Acknowledgements

For the completion of this work, I would like to express my thanks to supervisor Dr. Ali Mansourian for helpful advises and guidance during the project. Dr. David Tenenbaum that allowed me to implement new analysis. Especial thanks to Ajay Goel for inspiration to start this master, bright ideas and numerous hours we worked together to develop the algorithm. Also, thanks to Simarjit Singh, Theo Kaloumenos, Jan Reinholt and Lars Rasmussen for the help. Thanks to everyone at World Health Organization.

Thanks to Environmental Systems Research Institute (ESRI) and the spatial statistics team that provided some interesting website information with a description of the analysis tools used in this paper.

Thanks to my wife and kids for patience and support.

Abstract

The purpose of this work was to use spatial-temporal analysis for the prevention and mitigation of disease spread. A prototype application was specifically designed to detect territories with a high incidence of cases and a second was used to validate the results.

The first algorithm tried to find clustered cases territories and compare them to the average of the previous two years of data from the same places and their neighbors'. If more cases were detected based on a threshold, then it could be suspected that something unusual was happening. The application would detect such territories and provide alerts to health specialists. The second analysis for validation was using space time cubes method from Arc GIS Pro. It relied on Mann-Kendall and Getis-Ord statistics to detect hot spots territories.

The developed analyses have been applied in two cases studies: on the subnational level in Nigeria and in 53 countries belonging to the World Health Organization Regional Office for Europe (WHO Europe). For this reason, the Acute Flaccid Paralysis (AFP) surveillance data collected by the World Health Organization was used corresponding to two indicators: the total number of AFP reported cases and the total numbers of unvaccinated children.

The resulting reports have highlighted the underperforming regions in the North-East Nigeria and have spotted two previous outbreaks that occurred in WHO Europe: a large-scale polio outbreak in 2010 started in Tajikistan and a polio outbreak in Israel in 2013.

These space temporal analyses could be automatized to execute periodically and be incorporated into an outbreak prevention system. This would help detecting any future outbreaks.

Tables of contents

List of abbreviations

AFP	Acute flaccid paralysis
CISID	Centralized Information System for Infectious Diseases
ESRI	Environmental Systems Research Institute
GIS API	GIS Application Programming Interface
GIS	Geographic Information System
GPU	Graphics Processing Unit
IDW	Inverse Distance Weighted
LDMS	Laboratory Data Management System
Pol3	Third Dose of Polio containing vaccine
RCC	European Regional Certification Commission for Poliomyelitis Eradication
SACD	Smoothed Average Cluster Detection
SIA	Supplementary Immunization Activities
SOP	Standard Operational Procedure
STCDL	Space Time Cube for Defined Location
VDPV	Vaccine Derived Polio Virus
VPI	Vaccine-preventable Diseases and Immunization Programme of WHO
WHO Europe	World Health Organization Regional Office For Europe
WHO GEO	WHO Geographical database
WHO	World Health Organization
WPV1	Wild Polio Virus type 1
WPV2	Wild Polio Virus type 2
WPV3	Wild Polio Virus type 3

Lists of tables, figures and listing

1 INTRODUCTION

1.1 Purpose of the study

Population health is challenged by many infections such as polio, measles and rubella. The best way to fight these diseases is through prevention using vaccinations. Science has proven that vaccinations have the ability to improve our immune system and eventually eradicate these viruses.

Khetsuriani et al. (2014) said that the risk of any virus importation in a country or region depends on the following factors: population immunity, surveillance performance and outbreak preparedness. GIS technology could also be used to help prevent the outbreak of diseases.

The aim of this study is to use spatial analysis techniques to detect and analyze unusual patterns of polio in Nigeria and WHO Europe.

It will help to prevent and prepare for poliovirus outbreaks and detect places that require supplementary immunization activities (SIA). Considering that, many western countries in Europe have stopped reporting acute flaccid paralysis (AFP) data (Khetsuriani et al. 2014) and although, we are still collecting environmental and enterovirus information, still AFP clusters detections are critical for polio monitoring. The reintroduction of a wild poliovirus in these countries would have devastating consequences.

Therefore, a prototype to analyze clustered case patterns of polio cases will be created. It will help to prevent and give an early warning for possible future disease escalations. It will analyze two indicators: the total number of AFP reported cases and the total numbers of unvaccinated children (AFP zero dose).

Considering the aforementioned discussion above, the main objectives of this study are:

1. To identify the most vulnerable territories for polio in Nigeria and WHO Europe.

2. To analyze the spatial patterns of AFP zero dose cases in Nigeria and in WHO Europe for outbreak prevention purpose.

3. To describe how to incorporate the developed analyses in an outbreak prevention system.

The first aim is to develop a prototype for AFP case clustering which will be used in two case studies: to assess the situation in the aforementioned areas. The second aim is to analyze polio patterns, in those areas, using space-timed cubes for defined locations (STCDL).

1.2 Research questions

Based on the aforementioned issues the research questions are as follows:

1. Where are the territories most disease vulnerable to polio outbreaks located in Nigeria and the WHO European region?

2. What are the unusual GIS spatial-temporal patterns that could help prevent any future outbreaks?

3. How could we use the previous reported data to better understand or interpret current or future situations?

2 LITERATURE REVIEW

2.1 Case studies

According to WHO statistics, mortality cases due to a wild poliovirus, considered the most dangerous, have decreased by over 99% since 1988, from an estimated 350 000 cases then, to 22 reported cases in 2017. As a result of the global effort to eradicate the disease, more than 16 million people have been saved from lifelong permanent paralysis. There is no known cure for polio; it can only be prevented by using polio vaccine, given multiple times[1].

Speaking technically, there are three types of wild polio virus: Wild Polio Virus type 1 (WPV1), Wild Polio Virus type 2 (WPV2) and Wild Polio Virus type 3 (WPV3). In addition, there are very rare cases of vaccine derived polio (VDPV). The last detected WPV2 case was reported in 1999, and global eradication of WPV2 was certified in 2015. The last detected case of polio associated with WPV3 was reported in November 2012. The most recent case associated with WPV1 was reported in Nigeria[2].

Nigeria is a polio endemic country, together with Afghanistan, and Pakistan.

On 25 September 2015, Nigeria was classified as polio free, due to the fact that 12 months had passed since the last case[3]. Unfortunately, in 2016, four new cases of WPV1 and one case of VDPV were detected there, and the endemic country status was reintroduced.

Although the World Health Organization European Region (WHO Europe) was certified as polio-free in 2002 (Khetsuriani et al. 2014), there were still a number of polio virus importations in the region[4].

[1] WHO Poliomyelitis, key facts; http://www.who.int/news-room/fact-sheets/detail/poliomyelitis
[2] Report of the 30th Meeting of the European RCC for Poliomyelitis Eradication; http://www.euro.who.int/en/health-topics/communicable-diseases/poliomyelitis/publications/2016/30th-meeting-of-the-european-regional-certification-commission-for-poliomyelitis-eradication
[3] WHO Removes Nigeria from Polio-Endemic List; http://www.who.int/mediacentre/news/releases/2015/nigeria-polio/en/
[4] Factsheet Polio Euro, http://www.euro.who.int/__data/assets/pdf_file/0005/276485/Factsheet-Polio-en.pdf

There are many studies which have shown that GIS methods are effective to track and detect diseases clusters. However, the studies to date has tended to focus mainly on spatial analysis, spending less attention to the "time" dimension. Therefore, a prototype application was developed. Nevertheless, here will be discussed some of the case studies found in literature.

For instance a study for space time scanning was performed by Zhao (2013), exploring tuberculosis disease in China. He said, "Spatial clustering analysis can detect spatial autocorrelation when the values of variables at nearby locations are not independent from each other" (Zhao, 2013). This is also known as the Moran I test. He used SaTScan software for cluster detection. It is an open source software for spatial scanning created by Martin Kulldorff. Zhao used the SaTScan to create a seven-year time trend for clusters. Linear regression analysis was used to test the relationship between Global Moran I and time.

Tlou et al. (2017) performed a study about space-time child mortality in a rural area in South Africa whose population has a high HIV prevalence. In his case study he employed two techniques: Kulldorff spatial scan statistic SaTScan software using Poisson distribution and Tango spatial scan statistics implemented in FleXScan software. Tlou et al. (2017) also argued that Kulldorff's spatial scan uses a circular window to define the potential cluster areas and thus cannot detect irregularly shaped clusters, with the geographical distribution of health outcomes generally being non-circular. In addition, Tlou et al. (2017) said that FleXScan software is not practically feasible for larger cluster sizes, as it only works well for small to moderate clusters of up to 30 homesteads. To overcome this limitation his study area was divided on a grid with 705 cells.

Khetsuariani et. al (2014) have investigated the challenges of maintaining polio-free status in the WHO European region. They used AFP surveillance, environmental enterovirus surveillance and polio vaccination coverage to do an assessment of the risk of wild poliovirus spread following previous importations in the WHO European region. It categorized all countries as high, medium and low risk.

Mahar et. al (2016) performed a study for spatiotemporal pattern analysis of the incidence of scarlet fever incidence in Beijing, China. He used a Getis-Ord statistics from ArcGIS software, together with hot spot analysis to find the intensity and

stability hot spots of scarlet fever in his study area. He emphasized that this statistic based on confidence intervals is more accurate and provides much detailed information compared to SaTScan software that has a limitation for irregular geographic shapes. Mahar et. al (2016) have classified districts in two categories: with high Z-score (considered to be significant clusters at a 99% confidence level) and those with lower Z-scores (regarded with significance of 90% and 95%). This made it possible to classify clusters by significance. The current paper has used Getis-Ord statistics for analysis.

Ibrahim et. al (2015) had conducted an analysis of spatial pattern of the tuberculosis prevalence in Nigeria. He used Moran I test, Getis-Ord statistics and Invers Distance Weighting (IDW) interpolation to analyze spatial clusters and to predict their tuberculosis prevalence's. In his study, he concluded that Getis-Ord is more advantageous than Moran I since the first one allows pattern to be expressed as high or low clusters and contains much more information.

Other case studies outside public health have also been used to investigate space-time clustering. For example, a study conducted by Lixin [5], has used GIS cluster analysis to make the road safer. He had used space-time patterns and mapped traffic accidents using hexagon shapes on a grid in Brevard County, Florida USA. By performing a hot spot analysis and using mapped hexagons cells with statistical significance, he was able to identify clusters of roads with high rates of traffic accidents. Producing a 3D map of cubes allowed the results to be visualized. By understanding where and when traffic accidents occur throughout the county, Lixin[5] was able to make more informed recommendations for policies and other measures that could help reduce future traffic accidents.

A similar analysis was performed by Uittenbogaard et al. (2012) in Stockholm, Sweden. He tried to detect space-time clusters of crimes performed seasonally, weekdays and weekends. The Kulldorff Scan Test (SaTScan with Poisson model) has been chosen because it uses input data based on single events and is a software able to detect statistically significant clusters of point data. The results showed that the most likely clusters were located in the center of the city and that secondary clusters were

[5] Lixin Huang; *Analyzing traffic accidents in space and time*; http://desktop.arcgis.com/en/analytics/case-studies/analyzing-crashes-1-overview.htm

dispersed around the city. A-nova and Scheffe tests were used to test whether there was a significant difference in crime rates over time. Uittenbogaard et. al (2012) said that “knowing where and when crime happens is fundamental for police intervention”.

Abatan et al (2017) has performed an investigation on trends and variability in absolute indices of temperature extremes over Nigeria for the period 1971-2012. He had used Mann-Kendall trend test. It was a modified version that considered the effect of autocorrelation on the variance. He explained that this test is reliable and used in many researches to examine trends in hydroclimate time series. Abatan et al (2017) said that in order to avoid bias in mean values of trends in the indices, the mean results in each month were obtained by summing all the trends values and then divided by the total number of stations. This ensured that all months are given equal weight. His results, similar to previous studies on climate change has showed a significant warming trends in annual temperatures in Nigeria.

Elloit et. al (2004) has described the types of spatial epidemiologic inquiry: disease mapping, geographic correlation studies and disease cluster surveillance. Elloit et. al (2004) said that disease cluster surveillance could be incorporated into a proactive identification system using Kulldroff space-time pattern detection methods. It opens opportunity to provide early detection of raised incidences of disease even when there is no specific etiological hypothesis.

2.2 Clustering techniques

In this thesis, a special technique was designed by using the space time pattern method. Its purpose was to use previous reported data to find potential clusters in space and time. It would be applied in two case studies: Nigeria and WHO Europe.

This is particularly interesting from a health perspective, because in a situation of a disease outbreak an epidemiologist (health specialist) would start first looking for answers: Where are the clusters located? How wide is the spread? In other words: where are the borders and their neighbors? In the case of polio outbreaks, special supplementary immunization activities (SIA) are organized in affected territories and their neighbors. Oral polio vaccine is also administered to children. This has proven to be effective to stop the spread of polio. Of course, such situations need to be avoided.

To implement protective measures, space-time technique is a new and interesting solution that should be used to prevent such situations. Here some of the well-known techniques and tools will be reviewed.

A software (SaTScan) was designed by Kulldorff to do space scanning of clusters. Unfortunately, Tango (2005) in his study of flexible-shaped spatial scans for detecting clusters in the Tokyo Metropolis and the Kanagawa prefecture in Japan, had argued that Kulldorff 's SaTScan software uses a "circular window" with variable size to define the potential cluster area. It is difficult to correctly detect non-circular clusters such as those along a river. This limitation made the SaTScan software unusable for this paper, since study cases were spatially divided in defined locations of non-circular shape. In addition, Tango (2005) said that second software (FleXscan) was designed to do spatial scans to detect one small or medium cluster. (Since this paper analysis covers large territories with many clusters, it is also not suitable)

Both the SaTscan and the FleXScan software were tested and found to be unsuitable for current work. To fill these limitations, a prototype algorithm (Smoothed Average Cluster Detection SACD) was designed specifically for this paper. The next chapter contains a more detailed description of this algorithm.

Furthermore, scientifically proven techniques were needed to validate the SACD results. Doing a disease clustering review several methods were found that provide answers to these scientific questions. According to ESRI[6], these techniques could be categorized into the following three categories: *Analyzing patterns*, *Mapping cluster methods* and *Space time pattern mining*.

Analyzing patterns are general tests (using inferential statistics) designed to provide a single measure of overall patterns. They are based on the null hypothesis that there is no underlying pattern, or deviation from randomness, between the set of points (Rogerson, 2015). These include the following methods: Average Nearest Neighbor, High/Low Clustering, Incremental Spatial Autocorrelation, Multi-Distance Spatial Cluster Analysis (Ripley's k-function) and Spatial Autocorrelation.

[6] An overview of the Spatial Statistics toolbox; http://pro.arcgis.com/en/pro-app/tool-reference/spatial-statistics/an-overview-of-the-spatial-statistics-toolbox.htm

Rogerson also gave a detailed introduction using a Chi-square test, nearest neighbor test and Moran statistics (Rogerson, 2015).

All of the aforementioned tests are generally concerned with space clustering. In addition, some general tests specifically for space-time clustering detection were also found: Knox's, Mantel's and Jackquez's K-Nearest Neighbor tests (Tango, 2010). These methods frequently serve as a starting point for further analysis[7].

Mapping cluster methods, unlike the Analyzing patterns, which answer the question, "Is there spatial clustering?" with Yes or No, allows visualization of the cluster locations and their extent. These techniques help to find the answers to questions like: "Where are the clusters located?". For example, the first mapping technique ,also used in this paper, called the " Hot Spot" method utilizes a given set of weighted indicators and tries to identify statistically significant hot and cold spots using the Getis-Ord Gi statistic[5].

The second technique, density-based clustering classifies the strength of clustering (Figure 2-1). This method answers the question, "Where are incidents most dense?"

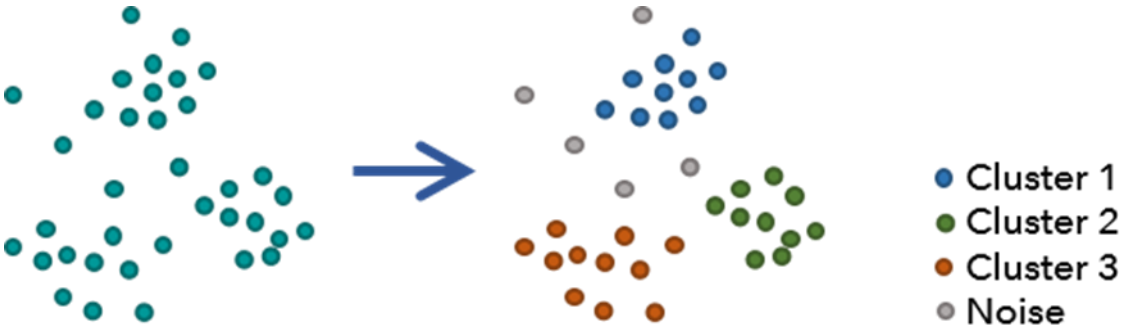

Figure 2-1: Classifying the strength of clustering. Source: ESRI

The third technique, cluster classification identifies spatial outliers. In other words, it tries to find anomalies (Figure 2-2). It answers the question, "Where are the spatial outliers?"

[7] ESRI; An overview of the Spatial Statistics toolbox; page 7

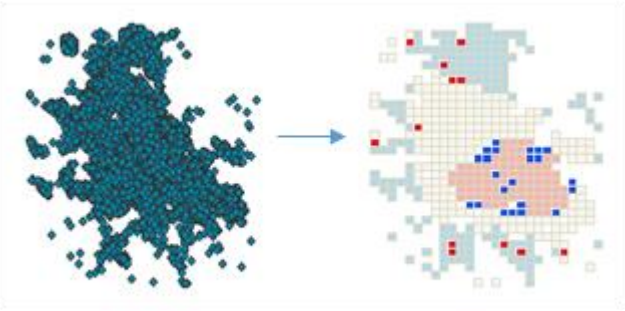

Figure 2-2: Finding spatial outliers. Source: ESRI

Finally, bringing time in space analysis (*Space Time Pattern mining*) has an interesting application. It helps to find patterns; explore relationships and understand temporal trends in data. It provides an understanding of the following questions: Where and when have things changed? Is it meaningful?[8].

An analysis has been developed using the Space Time Cube for Defined Location (STCDL). It relies on two statistical methods: Mann-Kendall and Getis-Ord Gi . The first one provides statistical significance of trends for clusters and the second one provides a scientifically proven way to detect and classify clusters.

In this paper, SACD tries to propose a new methodology for cluster identification, but STCDL will be used for verification of results. The difference between SACD prototype and STCDL is that first one searches for clusters using a threshold, but second one relies on scientifically proofed methods.

The next chapter contains a more detailed procedure to illustrate how STCDL techniques have been applied in this project and in following chapters discusses the validity of those results.

[8] ESRI; Spatial Statistics; https://spatialstats.github.io/presentations/

3 METHODS

The geographical and datasets used in this assignment were gathered from surveillance data reported to the WHO. Specifically, the case studies have been organized into two geographical areas: Nigeria and WHO Europe.

As the first step, all AFP cases data and geographical metadata have been imported in a Microsoft SQL database. The AFP cases have been aggregated (using date, time parameter and geographical location, space parameter) directly in the database and accordingly to the level of granularity needed for the analysis.

As the second step, as specified in the objectives, the data have been processed using Smoothed Average Cluster Detection (SACD) algorithm which tried to propose a new innovative methodology by using past reported data to detect cluster of cases in space and time. A second scientifically proven technique, Space Time Cube for Defined Location (STCDL) used a similar input data, but it's main purpose was to validate the results of the developed SACD prototype. These techniques will be described later in this chapter.

The above mentioned methods would use the following indicators: "Total AFP cases reported" and "Total AFP cases with zero doses". In order to prevent an outbreak, these indicators are important and need to be constantly monitored.

Finally, we will discuss how two algorithms could be incorporated into an outbreak prevention system for routine usage.

3.1 Available data

The first dataset consists of more than 64 000 cases collected for Nigeria. All these cases have a geographical location linkage with the WHO GEO database. The administrative level of Nigeria includes 37 provinces and 774 districts.

Only key variables from global WHO AFP dataset were made available for this work. The data did not contain any personal identifier and location information. Potential input for analysis are the date onset (time parameter), randomized with-in district geographical location of cases (space parameter), total number of AFP cases, total AFP cases with Zero doses, and the classification of a case (Table 3-1). These data have been reported since 2001. The current analysis will concentrate on the last five

years, during the 2013-2017 period, because more detailed information was provided for this interval. For years prior to this, most confirmed polio cases have been reported.

Table 3-1: Type of polio case classification, Source: WHO database metadata

Classification	Description
Confirmed Polio	Clinically or virologically confirmed poliomyelitis
Compatible	Possible vaccine-associated
Not an AFP	Spastic or chronic paralysis or facial paralysis only
VDPV	Vaccine derived polio virus
Discarded	Discarded as polio
Pending	The case results are under review

Similar to the Nigerian database, the second dataset consists of 19 476 cases collected from 53 member states in the WHO European region; unfortunately, the level of accuracy for case geographical location is lower compared to Nigeria. The surveillance site location is known for all of them. The report will aggregate all cases at the country level corresponding to the WHO European region.

In order to protect the personal data of patients, only aggregated numbers will be used for the analysis and presentation of results.

For simplicity, the absolute total numbers are used for analysis, meaning there are no population rates or percentages in the cluster detection.

3.2 Spatio-Temporal clustering analysis

There are a variety of methods to assess clusters. Each has its advantages and drawbacks, but the first law of geography states that “near things are more related than distant things”. Everything is related to everything else, but near (space) and recent things (time) are more related than distant things[9]. Hence, in this work both space and time parameters have been used to asses cluster importance. To statistically quantify the significance of clusters, the study area may be divided into a grid which

[9] ESRI; Spatial Statistics; page 9

resembles a fishnet, another in the shape of a hexagon, and locations defined by administrative borders

It was decided that searching for clusters in defined locations was a preferable method for this project, because the requirement from WHO was to use existing administrative boundaries. This would make planning for SIA activities much easier as borders did not change for time period used in the study areas. Also, explaining the results to decision makers would be easier.

Two case study areas were used in this thesis: Nigeria and the WHO European region. Nigeria is a polio endemic country and analysis would be performed at the district level. The WHO European region is a group of 53 countries where polio outbreaks happened in the past and the analyses were performed at the country level.

Moreover, two algorithms have been used to carry out the analyses. The descriptions of these methods are described below.

3.2.1 Design of Smoothed Average Cluster Detection (SACD) algorithm

The process of grouping and highlighting districts based on increased AFP reporting (or zero dose AFP reporting) in a given month provides the eradication program with an opportunity to detect and investigate the suspected outbreak situation.

The temporal grouping was carried out by executing the comparison of the current month's total with the average of the three month periods or segments from the previous two years. A minimum of three years worth of data was required to start the analysis.

To prepare the input data, AFP cases were collapsed by each district. This process was executed in the database. A simple query was performed to count the number of cases by locations. The input table is presented in Figure 3-1.

year	month	OBJECTID	nrc
2017	12	198	1
2017	12	201	5
2017	12	209	17
2017	12	214	14
2017	12	221	4
2017	12	228	2
2016	1	10	3
2016	1	13	2
2016	1	14	2
2016	1	19	4
2016	1	31	1
2016	1	78	2
2016	1	82	2
2016	1	101	4

Figure 3-1: Input data aggregated by year, month, OBJECTID (district code in the map) and Nrc(total number of cases in the district for specific month)

The next step in the workflow was the analysis of locations aggregated cases using the python application.

The program started to take each location polygon and identify its' neighbors. Furthermore, the algorithm calculates the number of cases in selected locations and its neighbors using three months averages for each year. For example, it started from current year: 2017 to 2016 and respectively 2015 (Figure 3-1).

Condition for Cluster sensitivity

(CYTotal > clusterSensitivity * PYTotal) or (CYTotal > (clusterSensitivity * PPYTotal))

Where variables are:
CYTotal - Current total 2017
PYTotal - Previous year total 2016
PPYTotal - Previous previous year total 2015
clusterSensitivity - Parameter for scale

Formula for calculation of variables:
CYTotal = Current district 2017 **Total** + each neighbour 2017 **Total**
PYTotal = Current district 2016 **Average Total** + each neighbour 2016 **Average Total**
PPYTotal = Current district 2015 **Average Total** + each neighbour 2015 **Average Total**

Total = SUM(month)
Average Total = SUM(AVERAGE(past month + current month + future month))
EACH MONTH WAS COMPARED TO AN AVERAGE OF 3 MONTH PERIODS IN THE PREVIOUS TWO YEARS

Listing 3-1: Condition for cluster sensitivity and variables notation

Next, the algorithm performed the comparison of district values and its neighbors. The situation in the current district was checked using the "Condition for cluster sensitivity" (Listing 3-1) which categorizes these as follows:

1. Potential outbreak – the area that has a higher number of aggregated cases compared to its neighbors in space and time.

2. Normal – areas where there is no significant deviation from the threshold (sensitivity parameter).

Subsequently, if the value were higher than the threshold defined by cluster sensitivity, then the polygon would be marked for further investigation. Values below the threshold were classified as normal.

Lastly, during the testing phase it was noted that locations with cases of outbreak often caused neighboring districts to be classified as possible zones of outbreak (when in fact, the cases of outbreak are quite low in reality).

In order to mitigate the influence of highly clustered districts to their neighbors it was decided to sort the districts, in descending order, by the number of cases. By running the SACD algorithm from the locations with the highest to lowest number of cases made it possible to remove locations that were already flagged (marked as potential

clustering) due to being in close proximity to districts where occurrences were strongest.

A description of the algorithm is presented in Listing 3-2.

0. Notations used in formulas

P – population of polygons with **aggregated number of cases by months** (ex. districts); $P \in (p_1, p_2 .. p_i)$

The population is ordered in descending order $p_1 \leq p_2 \leq p_2 .. \leq p_i$

N – neighbors of a **single polygon** p_i ; $N \in (n_1, n_2 .. n_j)$

Pcur – a **subset** of polygons for current year (ex. 2017); $Pcur \in (pcur_1, pcur_2 .. pcur_k)$

Ppy – a **subset** of polygons for previous year (ex. 2016); $Ppy \in (ppy_1, ppy_2 .. ppy_k)$

Pppy – a **subset** of polygons for previous previous year (ex. 2015); $Pppy \in (pppy_1, pppy_2 .. pppy_k)$

1. Calculation of totals for current year formula

$$\forall P(1,i), \forall Pcur(1,k), \quad \boldsymbol{CYTotal_i} = \sum_{m=1}^{12} pcur_{k,m} + \forall N(1,j) \sum_{m=1}^{12} \begin{cases} n_{j,m}\ marked\ , 0 \\ n_{j,m}\ not\ marked, n_{j,m} \end{cases}$$

2. Calculation of total for previous two years formulas

$$\forall P(1,i), \forall Ppy(1,k), \quad \boldsymbol{PYTotal_i} = \sum_{m=2}^{11} \frac{ppy_{k,m-1} + ppy_{k,m} + ppy_{k,m+1}}{3} + \forall N(1,j) \sum_{m=2}^{11} \begin{cases} n_{j,m}\ marked\ , 0 \\ n_{j,m}\ not\ marked, \frac{n_{j,m-1} + n_{j,m} + n_{j,m+1}}{3} \end{cases}$$

$$\forall P(1,i), \forall Pppy(1,k), \quad \boldsymbol{PPYTotal_i} = \sum_{m=2}^{11} \frac{pppy_{k,m-1} + pppy_{k,m} + pppy_{k,m+1}}{3} + \forall N(1,j) \sum_{m=2}^{11} \begin{cases} n_{j,m}\ marked\ , 0 \\ n_{j,m}\ not\ marked, \frac{n_{j,m-1} + n_{j,m} + n_{j,m+1}}{3} \end{cases}$$

3. Apply the clustering sensitivity condition for each location (ex. district or province)

$$ToMark\_p_i = (\boldsymbol{CYTotal_i} > clusterSensitivity * \boldsymbol{PYTotal_i}) \text{ or } (\boldsymbol{CYTotal_i} > clusterSensitivity * \boldsymbol{PPYTotal_i})$$

$$p_i\ classification \begin{cases} ToMark\_p_i = True, & mark\ p_i \\ ToMark\_p_i = False, & not\ mark\ p_i \end{cases}$$

Marked polygons are those with potential outbreak.

Listing 3-2: SACD description of the algorithm

The prototype exported results as shape files. This output can be visualized and modified for example using the ArcGIS Map or others software.

The data workflows of this algorithm were presented in Listing 3.3. In summary, the data was aggregated. (Listing 3.3 step 1 and 2). Then, the python application (Listing 3.3 step 3) used Arc GIS API to execute the SACD analysis. It outputs results into an Arc GIS shape file format, that can easily be visualized and modified (Listing 3.3 step 4 and 5).

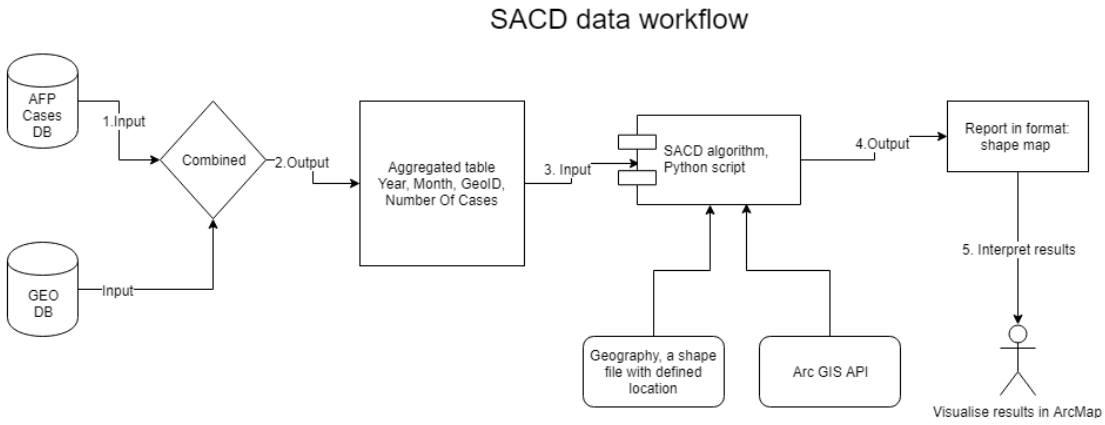

Listing 3-3: Data workflow for SACD method

3.2.2 Space Time Cube for Defined Location (STCDL) implementation

A cube is a collection of AFP polio cases that are near each other in space and time. In this method each defined location has a cube corresponding to each time period. For example, there are 53 countries in WHO Europe and if past ten years were analyzed, then there would be 530 cubes in this study area.

The Space Time Cube for Defined Location (STCDL) analysis tried to find correlations, if a cube and its neighbors are significantly different from rest of cubes in the study (Figure 3-2).

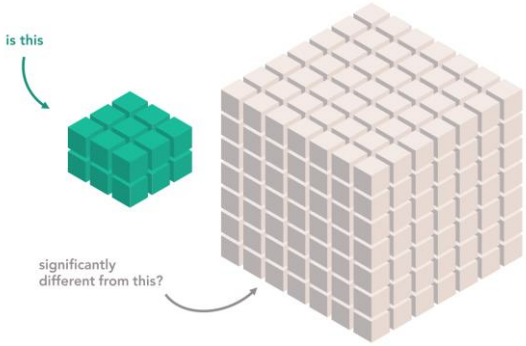

Figure 3-2: Correlations between selected neighbors and population Source: ESRI

Each selected cube has neighbors in space (Figure 3-3) and in space-time (Figure 3-4). The neighbors in space are located on X, Y axes and time neighbors are on Z (time axes), Figure 3-4.

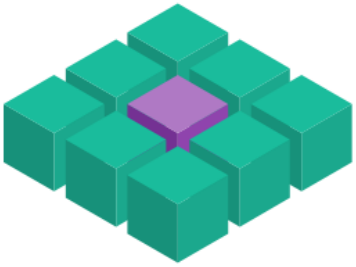

Figure 3-3: A cube (purple) with its neighbors in space Source: ESRI

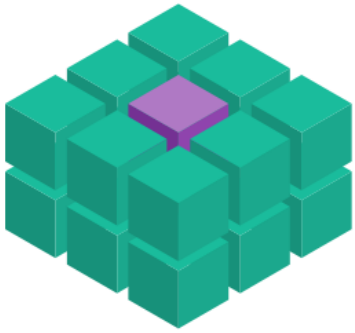

Figure 3-4: A cube (purple) with its neighbors in space and time Source: ESRI

In other words, the points (AFP cases) have been aggregated in cubes (Figure 3-5). The points were gathered in cubes (bins, in other literature) that were near each other in time and space, X corresponding to longitude and respectively Y- to latitude. For easy visualization the time and distance parameters were shown on the cube axis in Figure 3-6.

A new method was introduced in the software ArcGIS Pro, called Space Time Cube for Defined Locations (STCDL), because it met WHO requirements. It used Mann-Kendall statistics that took into account administrative borders, along with past information to produce a spatial analysis for potential outbreak prevention. In addition, it calculated the Getis-Ord Gi statistics for the hot spot analysis. The resultant z-scores and p-values tell you where there were features with either high or low values cluster spatially[10].

[10] How Hot Spot Analysis (Getis-Ord Gi) works; http://pro.arcgis.com/en/pro-app/tool-reference/spatial-statistics/h-how-hot-spot-analysis-getis-ord-gi-spatial-stati.htm

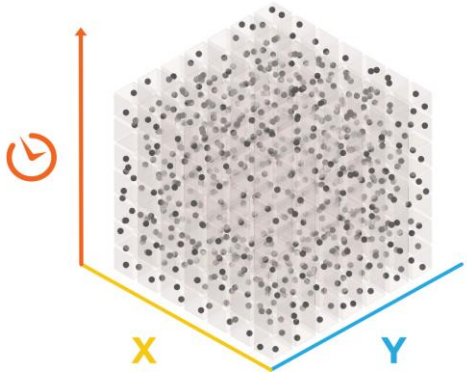

Figure 3-5: Location and time axes Source: ESRI

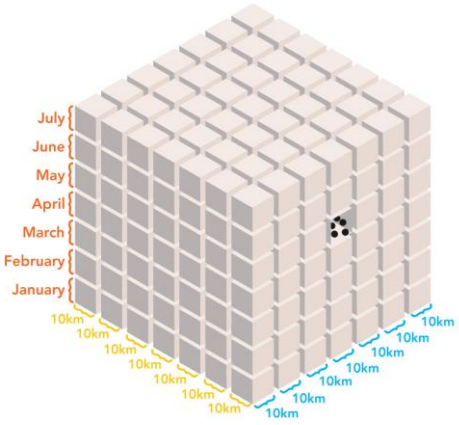

Figure 3-6: Axes parameters Source: ESRI

Depending on the method used, cubes filled with point data could be attached to the fishnet grid, hexagon grid or a newest approach - defined locations (Figure 3-7). As explained before, in this paper, the defined locations option has been used.

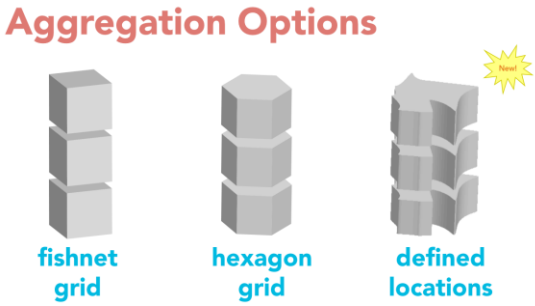

Figure 3-7: Different type of cubes analysis Source: ESRI

After running the space-time aggregation function, these cubes were organized in a special data structure - network Common Data Form (NetCDF).

NetCDF is a self-describing, machine-independent data format that supports the creation, access, and sharing of array-oriented scientific data[11].

Furthermore, during the cubes initialization the time trend is calculated. It relies on Mann-Kendall statistics[12]. It is a non-parametric test for identifying trends in times series. One benefit of it is that data does not require confirmation to any particular distribution shape.

The Mann-Kendall trend test was performed on every location with data as an independent cube time-step test. The Mann-Kendall statistic is a rank correlation analysis for the cube count or value and their time intervals[13]. The cube value for the first time period was compared to the cube value for the second. If the first was smaller than the second, the result was a +1. If the first was larger than the second, the result was -1. If the two values were tied, the result was zero. The results for each pair of time periods compared were summed. When expected sum was zero, indicating no trend in the values over time. Based on the variance for the values in the cube time series, the number of ties, and the number of time periods, the observed sum was compared to the expected sum (zero) to determine if the difference was statistically significant or not.

The trend for each cube time series was recorded as a z-score and a p-value. A small p-value indicates the trend was statistically significant. The sign associated with the z-score determines if the trend was an increase in cube values (positive z-score) or a decreased in cube values (negative z-score)[11].

Formally, the initial value of the Mann-Kendall statistic S, was assumed to be 0 (no trend). If a data value from a later time period was higher than a data value from an earlier time period, S was incremented by 1. On the other hand, if the data value from a later time period was lower than a data value sampled earlier, S would be decremented by 1. The net result of all such increments and decrements yields the final value of S[11].

[11] NetCDF Fact Sheet;
https://www.unidata.ucar.edu/publications/factsheets/current/factsheet_netcdf.pdf
[12] Khambhammettu Prashanth; Mann-Kendall statistics memorandum;
http://www.statisticshowto.com/wp-content/uploads/2016/08/Mann-Kendall-Analysis-1.pdf
[13] "How Creating a Space Time Cube works"; http://pro.arcgis.com/en/pro-app/tool-reference/space-time-pattern-mining/learnmorecreatecube.htm

Let $x_1, x_2, \ldots x_n$ represent n data points where x_j represents the data point at time j. The Mann-Kendall Statistics (S) is as following:

$$S = \sum_{k=0}^{n-1} \sum_{j=k+1}^{n} sign(x_j - x_k)$$

$$sign(x_j - x_k) \begin{cases} 1, & x_j - x_k > 0 \\ 0, & x_j - x_k = 0 \\ -1, & x_j - x_k < 0 \end{cases}$$

A very high positive value of S is an indicator of an increasing trend, and a very low negative value indicates a decreasing trend. However, it is necessary to compute the probability associated with S and the sample size n.

$$VAR(S) = \frac{1}{18}\left[n(n-1)(2n+5) - \sum_{p=t}^{g} t_p(t_p - 1)(2t_p + 5)\right]$$

Where n is the number of data points, g is the number of tied groups (a tied group is a set of sample data having the same value), and t_p is the number of data points in the p^{th} group[14].

A normalized test statistics Z could be computed as follows [13]:

$$\begin{cases} S > 0, Z = \dfrac{S-1}{[VAR(S)]^{1/2}} \\ S = 0, Z = 0 \\ S < 0, Z = \dfrac{S+1}{[VAR(S)]^{1/2}} \end{cases}$$

Visually, when STCDL analysis have been executed, it iterated each cube, found the space-time neighbors (Figure 3-8) and calculated the significance of the cube. An example result is show in Figure 3-9.

[14] Khambhammettu Prashanth; Mann-Kendall statistics memorandum; Page 20

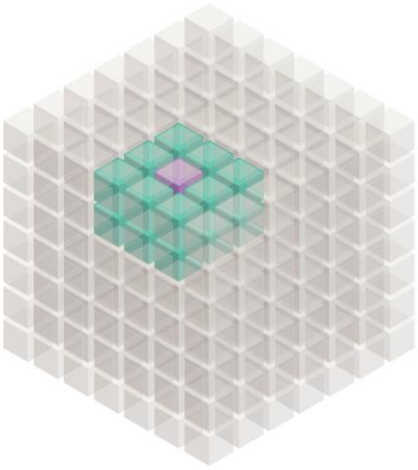

Figure 3-8: Example of one cube iteration Source: ESRI

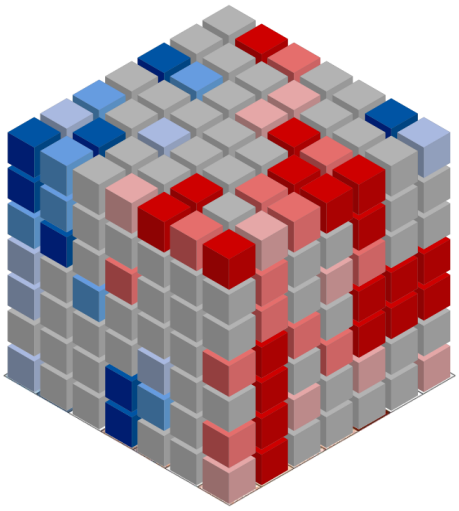

Figure 3-9: Example of results with all classified cubes Source: ESRI

Finally, the hot spot analysis technique, classified the space-time cubes into a summary layer, shown in figure 3-10. There are 12 categories (Figure 3-10) in the classification from “new hot spot” to “no trend detected”. An example of space-time analysis (yellow circle in figure 3-10) classified as “sporadic hot spot” because, over time it was changing state from cold and hot spots and in last cube, it was a new hot spot.

Also, for identification of hot spots the Getis-Ord local statistics was used. As a prerequisite for the calculation of Getis-Ord local let’s consider that:

x_j is the attribute value for feature j

$w_{i,j}$ is the spatial weight between feature i and j

n is the total number of the features.

$$\bar{X} = \frac{\sum_{j=1}^{n} x_j}{n}$$

$$S = \sqrt{\frac{\sum_{j=1}^{n} x_j^2}{n} - (\bar{X})^2}$$

The Getis-Ord local is calculated as following:

$$G_i = \frac{\sum_{j=1}^{n} w_{i,j} x_j - \bar{X} \sum_{j=1}^{n} w_{i,j}}{S \sqrt{\frac{\left[n \sum_{j=1}^{n} w_{i,j}^2 - \left(\sum_{j=1}^{n} w_{i,j} \right)^2 \right]}{n-1}}}$$

The G_i for each feature in the dataset is a z-score. For statistically significant positive z-scores, the larger the z-score is, the more intense the clustering of high values or hot spot. For statistically significant negative z-scores, the smaller the z-score is, the more intense the clustering of low values or cold spot[15].

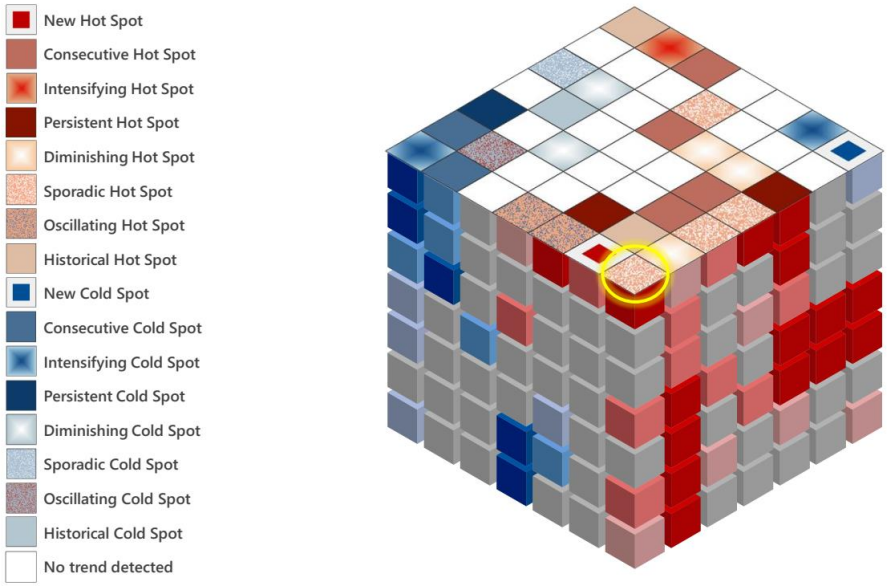

Figure 3-10: Final results classification Source: ESRI

A data workflow for STCDL analysis was showed in listing 3.4. In summary, the aggregated by location AFP cases were combined with geographical locations features the NetCDF cubes structure was created. Then a "Emergency Hot-spot

[15] How Hot Spot Analysis (Getis-Ord Gi) works; page 18

analysis" and classification analysis was processed. In the final step the geographical data was again merged with classified Hot-spot analysis and visualized as 3D shapes.

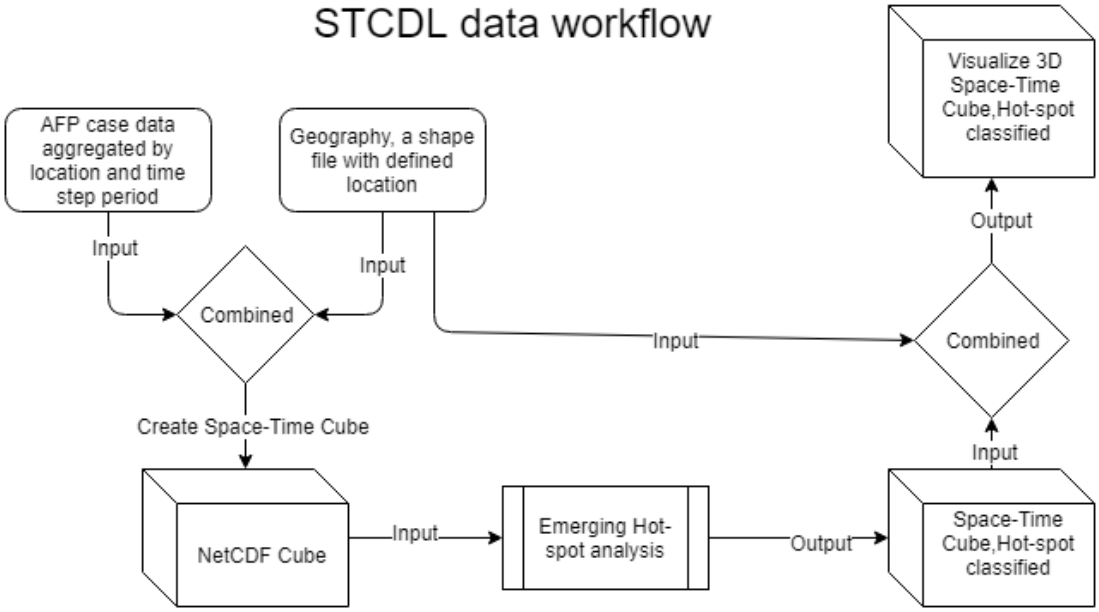

Listing 3.4: Data workflow for STCDL method

4 RESULTS

4.1 Case study Nigeria

4.1.1 Analysis of AFP cases, SACD results

Maps displayed in figure 4-1 and 4-2 show the districts highlighted using the SACD algorithm. It presented how polio disease has evolved over a five years period in Nigeria. In the first series of maps (Figure 4-1), a cluster sensitivity parameter of 30 was used.

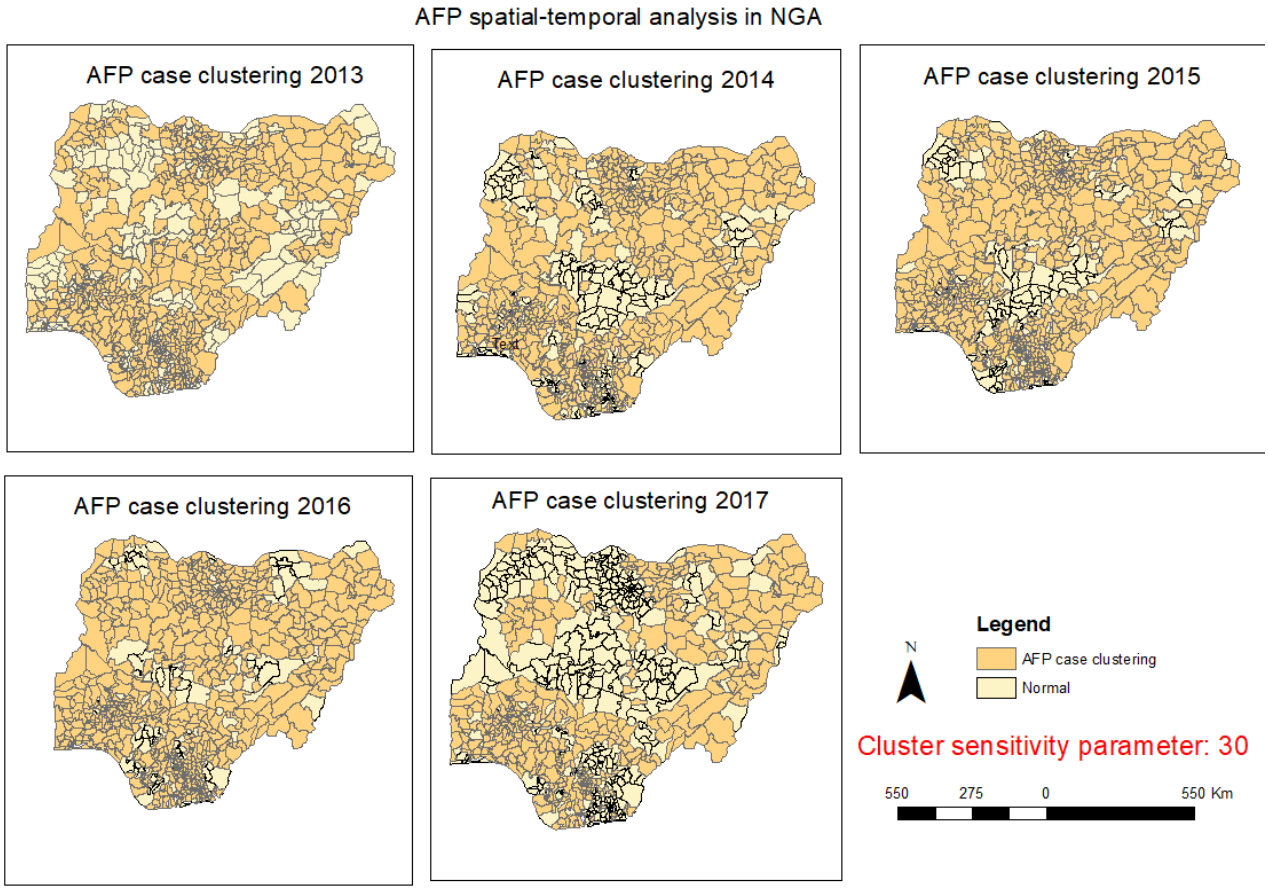

Figure 4.1: Nigeria, spatial-temporal analysis, cluster sensitivity parameter: 30

These highlighted territories were indeed low performing districts and suffered with multiple polio outbreaks in the past. In addition, the data was validated from the graph in figure 4-3. It shows that the number of cases has consistently increased since 2010 (5988 AFP cases) and peaked in 2016 (17865 AFP cases). It had dropped by 3747 cases in 2017. Considering that the input data for the year 2017 was only partially available and including up to September 2017, this was an expected behavior.

Furthermore, to analyse the clusters of cases, the sensitivity parameter was increased to 100 and derived a second series of maps (Figure 4-2). All clustered districts (Figure 4-2) were included also in the previous series of maps (Figure 4-1). These districts had an increase of more than 100 times compared to the previous two years. As a result, the clusters of high cases became even more evident.

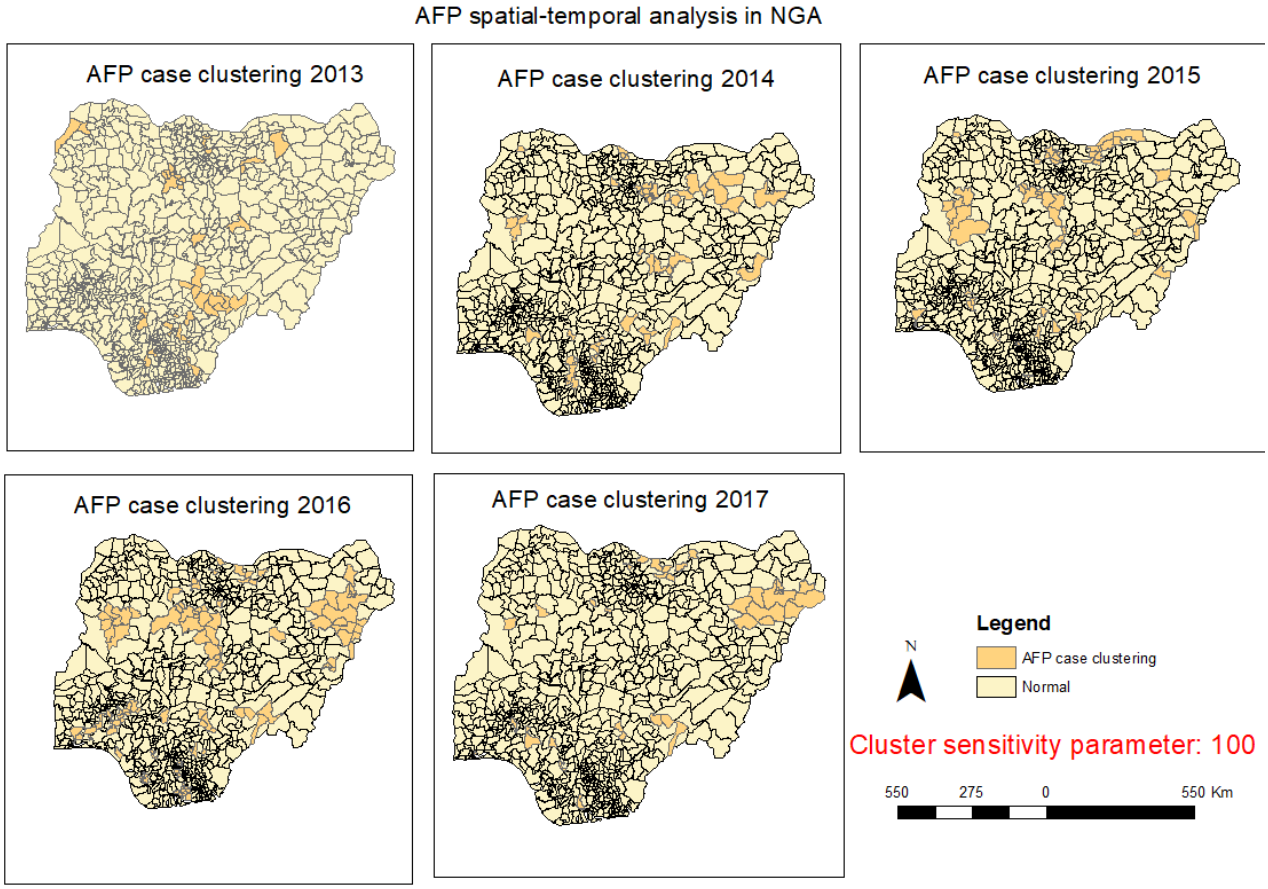

Figure 4.2: Nigeria, spatial-temporal analysis, cluster sensitivity parameter: 100

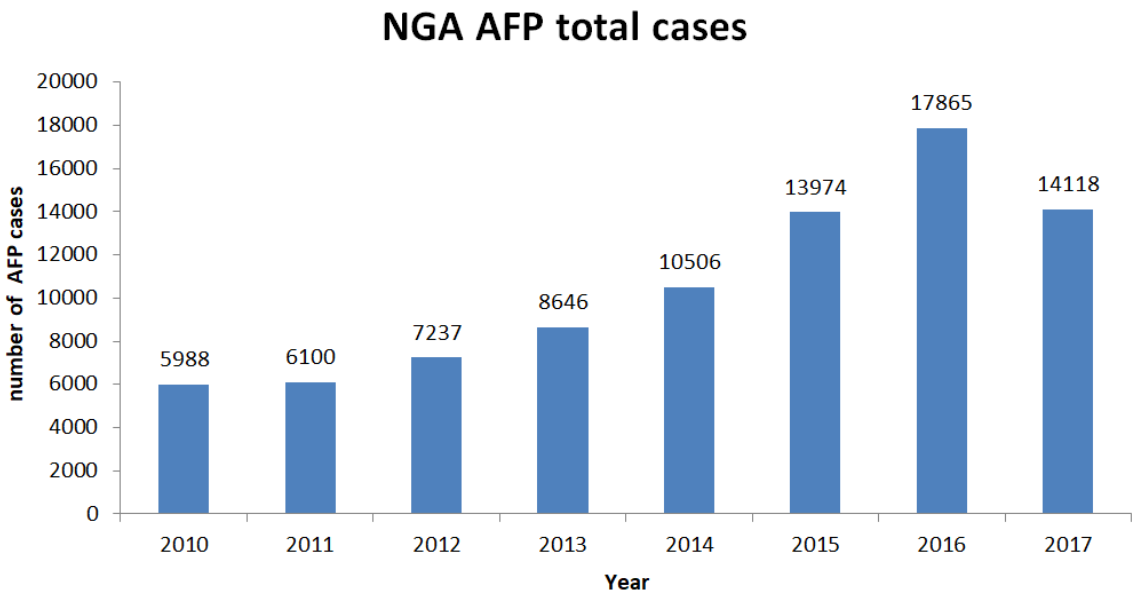

Figure 4.3: Nigeria, distribution of total AFP cases by years

4.1.2 Analysis of AFP cases, STCDL results

As explained in the methods chapter, the first part in the STCDL analysis involved creating a space time cube (NetCDF structure) for defined locations. In addition, the STCDL analysis imposed a requirement of a minimum 10 time steps. To solve this issue, six months steps instead of yearly were chosen, which resulted in ten cubes per location (ten time steps). The analysis still covers five years.

The mean was used as a parameter for case aggregation. The neighbors in space and time were used to predict districts that could not be estimated from input data.

This analysis consists of all population AFP cases in Nigeria and is not a fraction sample. These means that the statistics represent facts for the population and not a prediction. The overall Mann-Kendall data trend for the analyzed variables was increasing with a p-value equal to 0,0042 and trend statistics of 2,8622. A low p-value means that there is a significant trend. The full STCDL summary information was displayed in appendix, Figure A-1.

The results of hot spot analysis were presented in Figure 4-4.

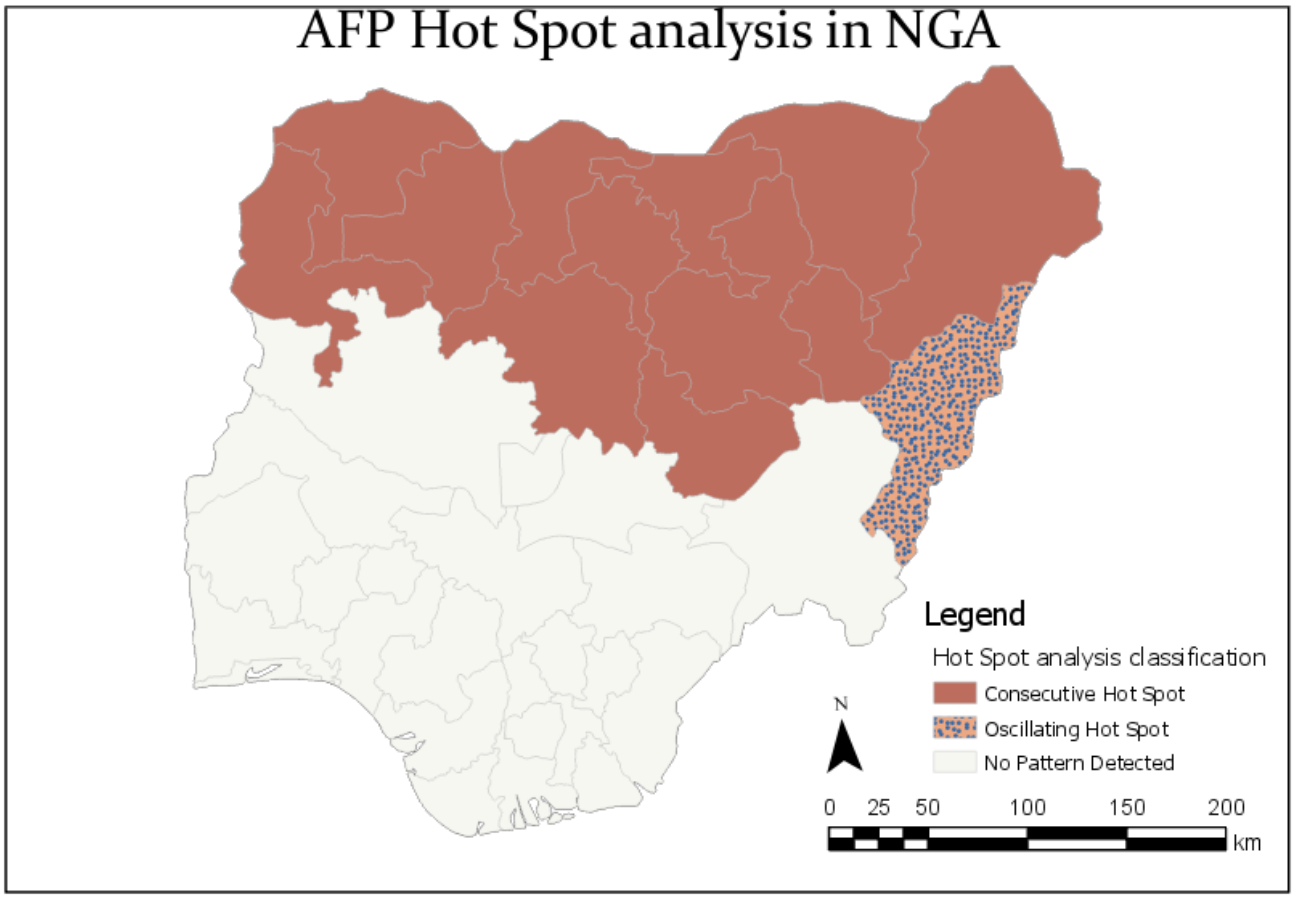

Figure 4-4: Nigeria, AFP Hot Spot analysis

All territories (Figure 4-4) were classified into the following three categories: *consecutive hot spot*, *oscillating hot spot*, areas where *no pattern was detected*

It is clearly visible from figure 4-5 that many territories in the North of Nigeria were classified as a *consecutive hot spot*, because they had a high number of cases in final time-steps (note top cubes colored in red figure 4-5).In other words, a consecutive hot spot was defined as a single uninterrupted run of statistically significant cubes in the final time-step intervals (in this study final steps were in 2016,2017 years). Also, these locations have not been statistically significant hot spot prior to the final hot spot year and less than ninety percent of all cubes are statistically significant hot spots[16].

In the figure 4-5, one province on the North-East side was classified as *oscillating hot spot* because like the previous category "consecutive hot spot" the last cubes were statistically significant hot spots for the final time-step interval and in addition, it had

[16] "How Emerging Hot Spot analysis work"; http://desktop.arcgis.com/en/arcmap/10.3/tools/space-time-pattern-mining-toolbox/learnmoreemerging.htm

a time step classified cold spot (blue color cube). In other words, this province has been switching between hot and cold spots[17].

The last category, *no pattern detected* indicates that these territories do not fall in any of the 12 categories of the hot or cold spots classification.

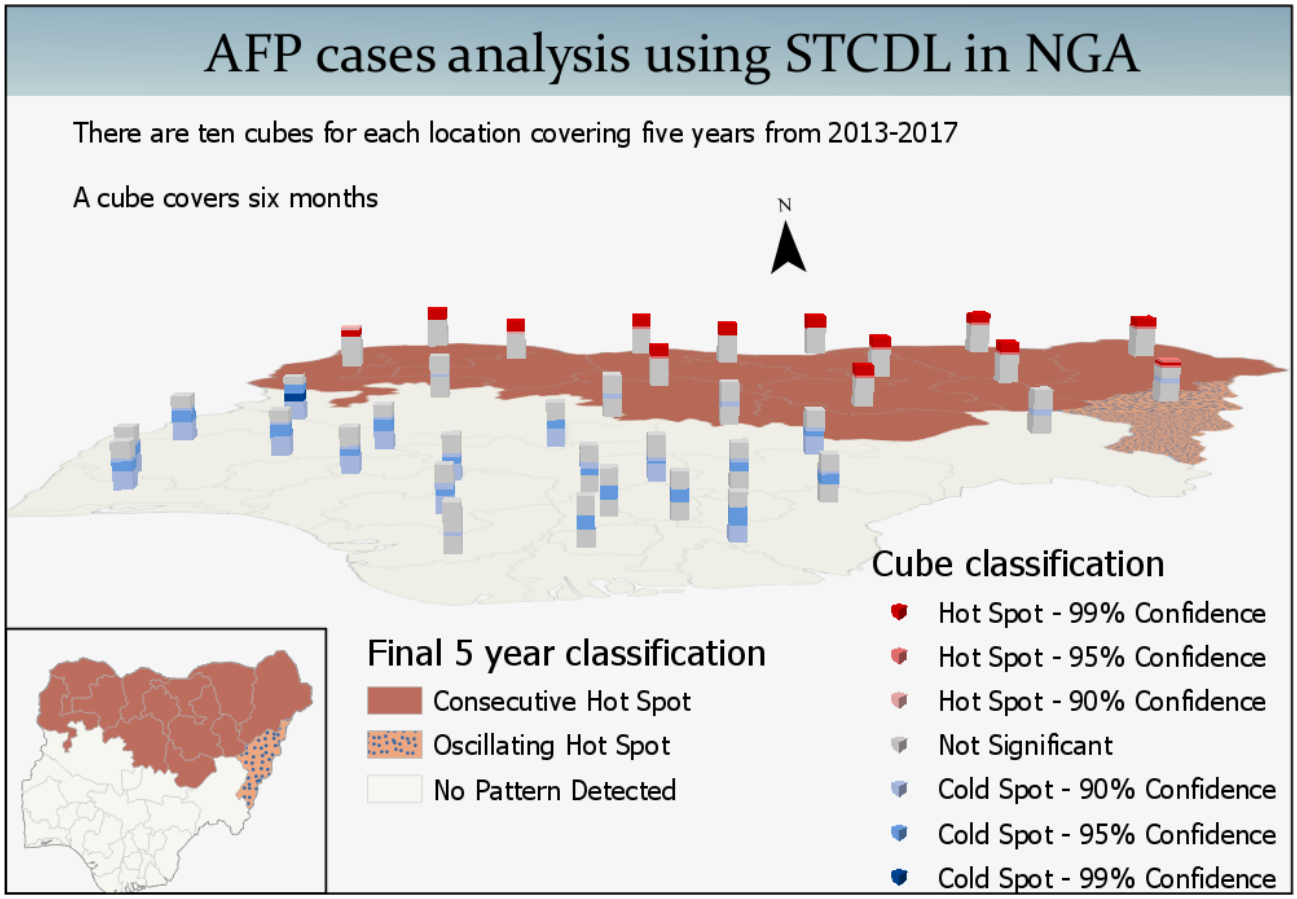

Figure 4-5: Nigeria, AFP cases analysis using STCDL using mean for aggregation

It is also possible to create the cubes using the sum of the cases rather than the mean as in the previous example.

The results looks almost the same with an increasing trend direction and a statistical value of 1,9677 and a p-value 0,049, which is in within the 95% confidence interval.

The results and classification of the cubes were presented in figure 4-6. There were two categories similar to the previous analysis. The only difference was that one

[17] "How Emerging Hot Spot analysis work"; page 28

location that was previously classified as an oscillating hot-spot, was classified as having no pattern in this analysis.

Appendix figure A-2 showed the detailed summary table for the cubes creation.

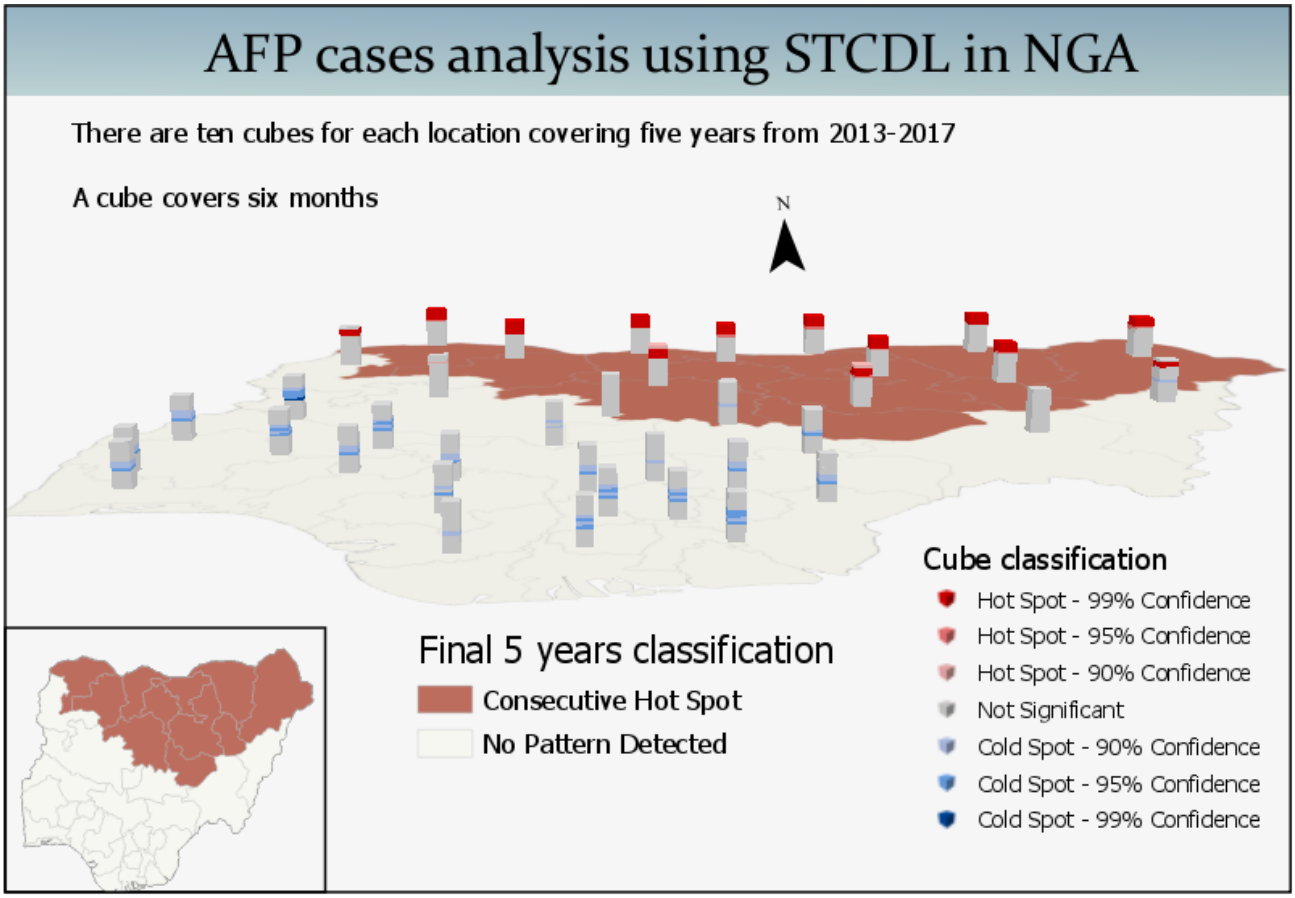

Figure 4-6: Nigeria, AFP cases analysis using STCDL using sums for aggregation

4.1.3 Analysis of zero dose cases, SACD results

An essential and interesting analysis was to detect the location of cases with zero doses. This was a very important analysis, as every child counts especially in a polio-endemic country like Nigeria.

The number of cases with zero doses were presented in the figure 4-7. We detected a sharp decline from 231 in 2010 to 47 in 2016 and 51 in 2017. This decrease was a consequence of many SIA activities in the country.

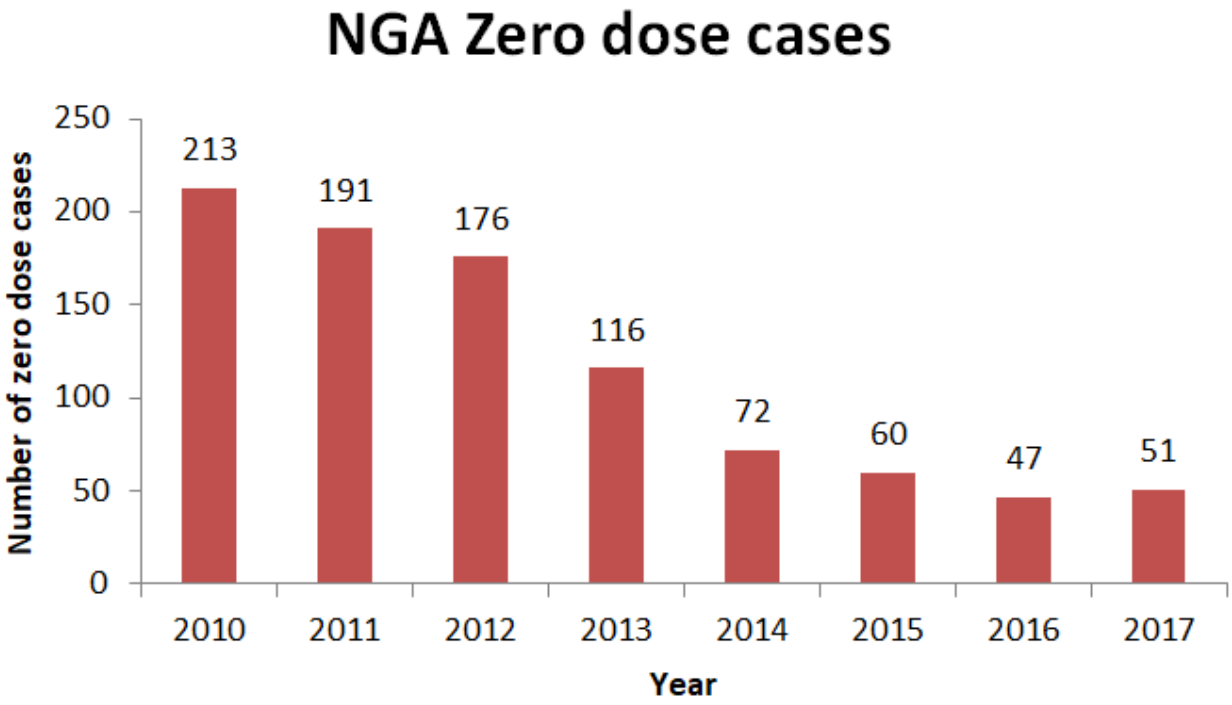

Figure 4-7: Nigeria, distribution of zero dose AFP cases by years

The algorithm was run with zero dose cases as input. These results were presented in figure 4-8, 4-9 and 4-10. The sensitivity parameter was important to be accommodated to amount of input data. In this scenario, only a small fraction (total of 926 zero dose cases) were used from total of 64 000 cases used in the previous analysis, therefore the sensitivity parameters were much smaller. They were set to 2, 3 and 5 in figure 4-8, 4-9 and 4-10 respectively.

One important aspect of the SACD algorithm, is that cluster of cases in a defined location could be significant only if it exceeds the total of reported cases in same period of past year multiplied by cluster sensitivity parameter. In other words, a cluster parameter of 2 means twice as big compared to previous year or 100 means one hundred times as big compared to previous year.

In the maps shown in figure 4-8, there was a gradual decrease in the number of selected districts from 2013 to 2016. These districts had twice the number of zero dose cases compared to the previous two years. These allowed us to make a conclusion, that the most vulnerable districts were located in the North-East part of Nigeria.

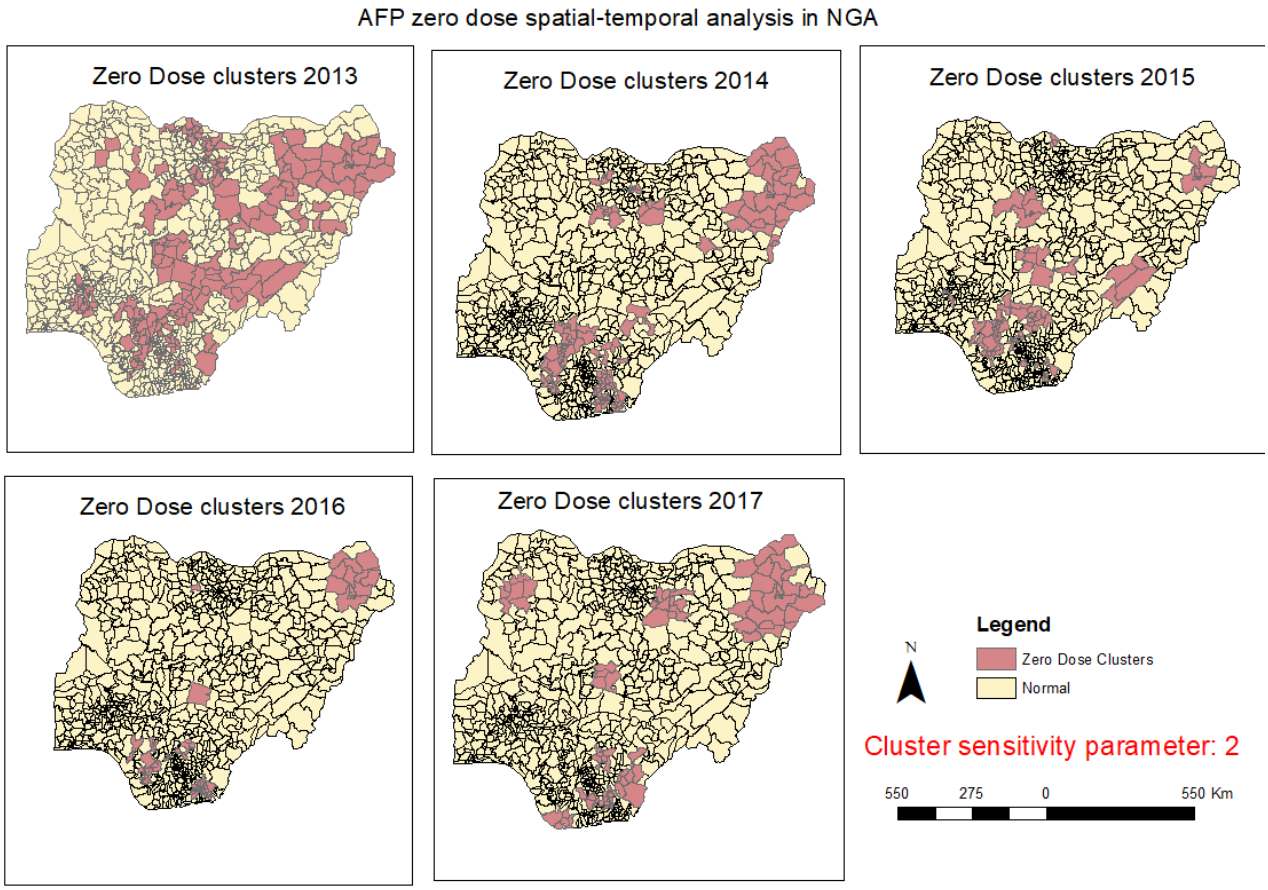

Figure 4-8: Nigeria, AFP zero-dose cases analysis using SACD, cluster sensitivity parameter: 2

In figure 4-9, the cluster sensitivity parameter was slightly increased from 2 to 3. It was now more illustrative that a cluster in North-East of the country was more distinct.

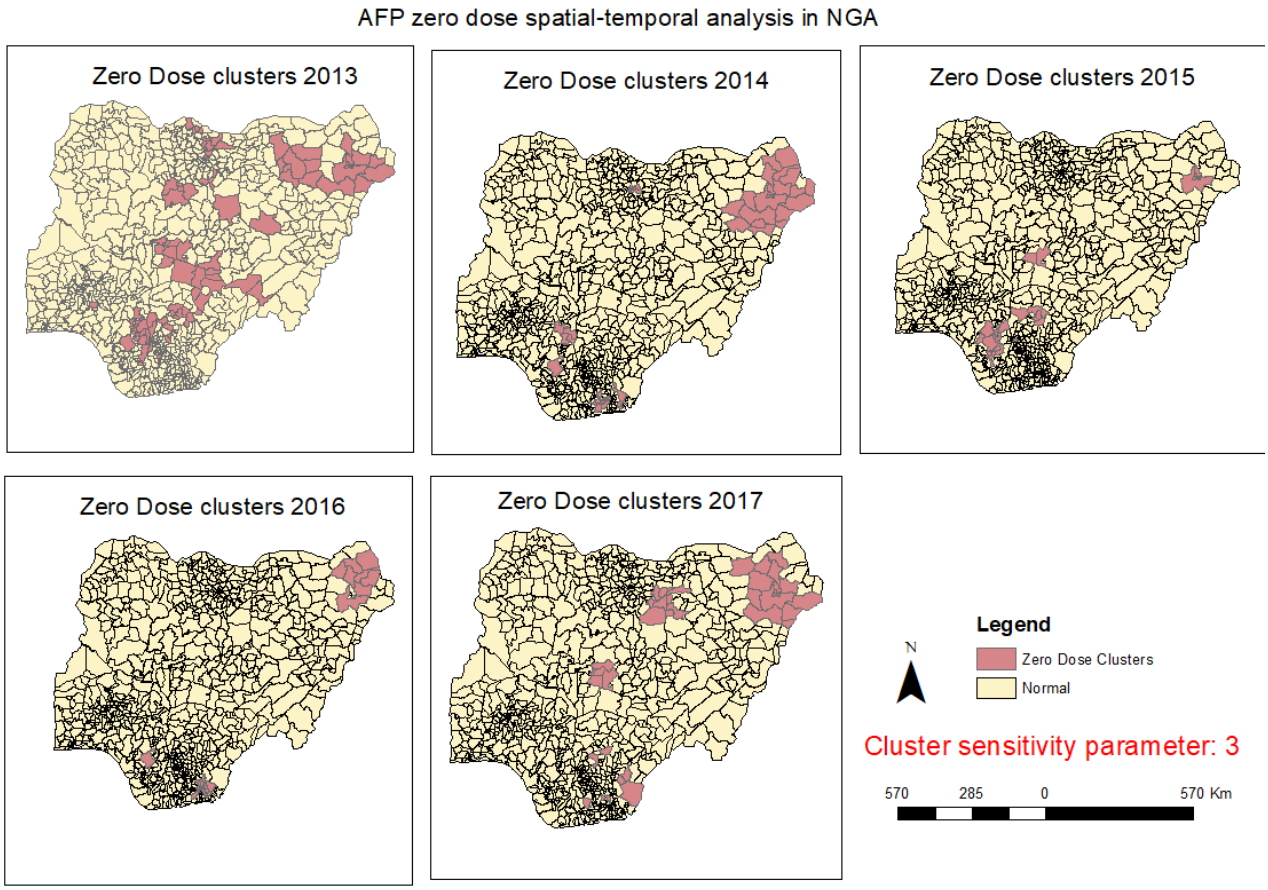

Figure 4-9: Nigeria, AFP zero-dose cases analysis using SACD, cluster sensitivity parameter: 3

In the last analysis (Figure 4-10), the cluster sensitivity parameter was increased to 5. Again, the clustering in the North-Eastern part of the country was confirmed.

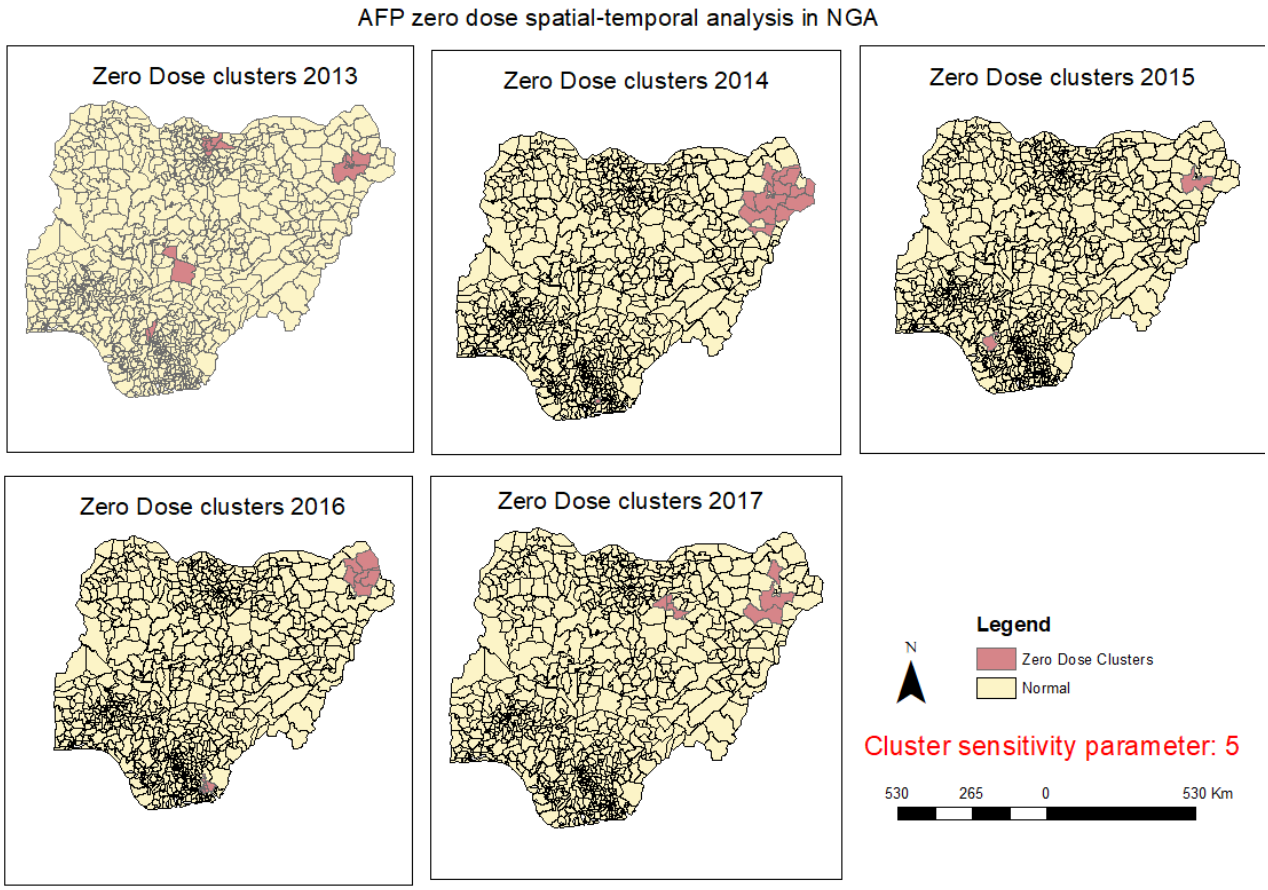

Figure 4-10: Nigeria, AFP zero-dose cases analysis using SACD, cluster sensitivity parameter: 5

4.1.4 Analysis of zero dose cases, STCDL results

The NetCDF structure for STCDL of zero dose cases analysis has been created. As in a previous analysis, the six months steps were used for last five years, resulting in ten cubes per location. The Mann-Kendall trend statistics resulted in a insignificant trend. The p-value is 0.5296 and the trend statistics is -0.5410. It would have been a negative trend, but since the p-value was so high, the trend has been classified as insignificant. The full summary information was presented in figure A-3.

The final hot spot analysis classification and cubes were presented in figure 4-11.

For most of the area, there was no pattern detected, but for the North-East part of the country a “Sporadic Hot Spot” was detected. This coming and going hot spot behavior was visible in cubes from the North-East part of the country

In other words, it was classified as a location that was an on-again then off-again hot spot. Less than ninety percent of the time-step intervals have been statistically

significant hot spots and none of the time-step intervals have been statistically significant cold spots[18]. It was interesting to notice a similar behavior in the North-East part in the map from the SACD algorithm presented earlier.

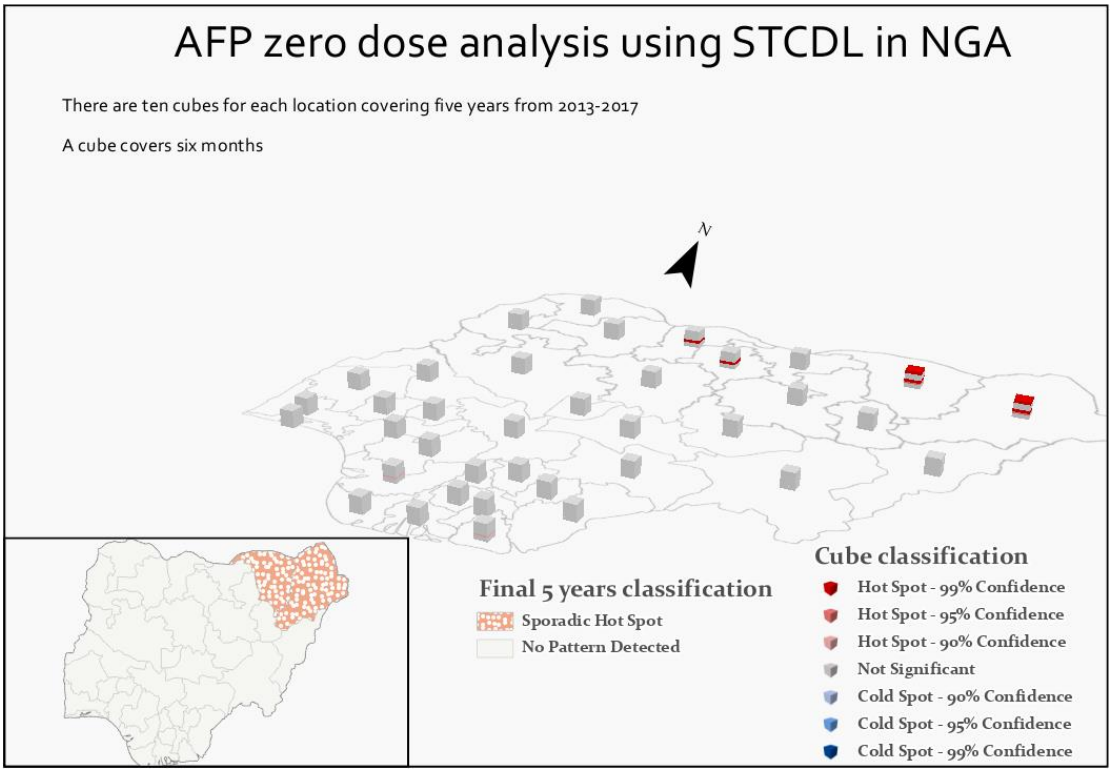

Figure 4-11: Nigeria, AFP Zero cases analysis using STCDL, using sum for aggregation

4.2 Case study WHO Europe

4.2.1 Analysis of AFP cases, SACD results

The WHO European region had the last indigenous case of poliomyelitis in 1998 and was certified as polio free by the European Regional Certification Commission for Poliomyelitis Eradication (RCC) in 2002 (Khetsuriani et. al 2014).

Nevertheless, it had fewer AFP cases compared to Nigeria and therefore, the parameters for cluster sensitivity were lower. The SACD analysis results were displayed in figure 4-12 and 4-13. The cluster sensitivity parameter was set to 40 and respectively 50. The data for the past 10 years (2007- 2017) was analyzed, but since the SACD requires data for minimum past two years the first report started in 2009.

[18] "How Emerging Hot Spot analysis work"; page 28

An important cluster of cases in the South-East part of the region has been detected in 2010. This is significant because, a large-scale outbreak occured in 2010. It had started in Tajikistan caused by the introduction of WPV1 of Indian origin (Khetsuriani et. al 2014) and spread to neighboring countries: Russian Federation, Turkmenistan and Kazakhstan. In the presented results, Turkmenistan and Kyrgyzstan did report a large number of AFP cases in 2010.

Luckily, after large scale SIA activities, the virus transmission was stopped in the same year and WHO Europe kept its polio free status. Please note that, Tajikistan continued to report a large number of AFP cases in the following years 2011-2013 (Figure 4-12).

In addition is worth mentioning that there was a significant cluster of AFP cases in Israel in 2013. Both cluster sensitivity parameters of 40 and 50 have detected the trend. It was caused by an importation of WPV1 into the Gaza Strip and West Bank. WPV1 of Pakistani origin was detected in sewage samples. No cases of paralytic polio were reported (Khetsuriani et. al 2014).

There were clusters detected in the south of the WHO European region: Bulgaria and the Republic of Macedonia in 2009 and Serbia in 2013. According to risk analysis, these countries were classified as low risk (Khetsuriani et. al 2014) and no major outbreaks have been reported from these countries. There were no patterns detected in years 2014-2017.

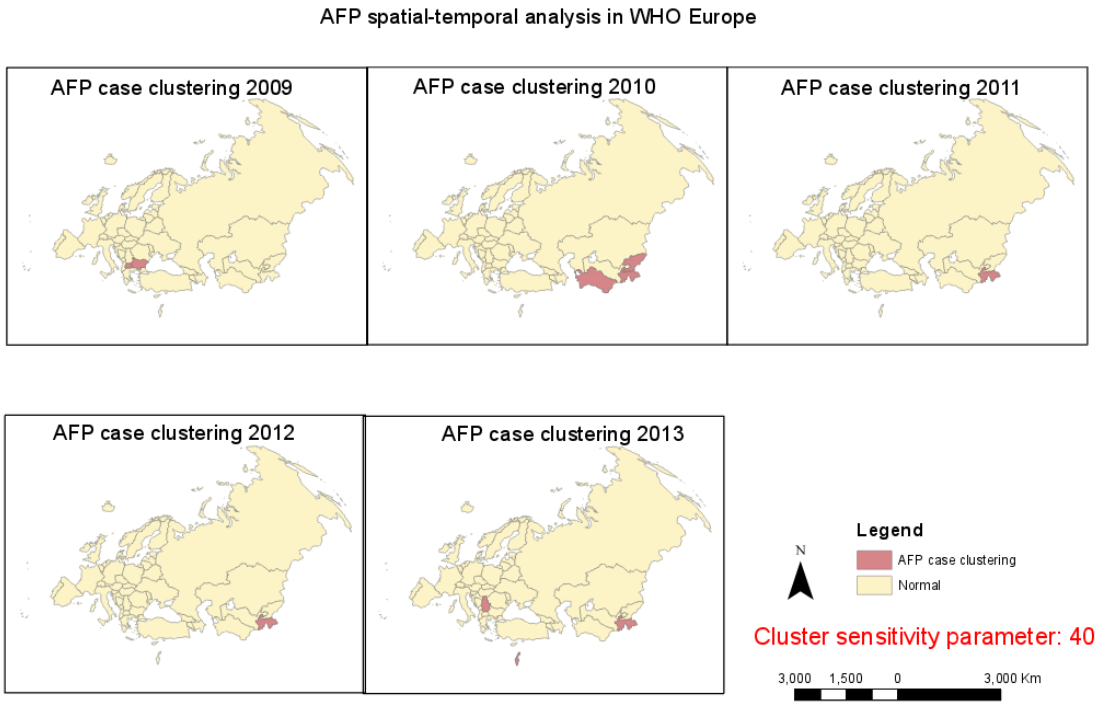

Figure 4-12: WHO Europe, spatial-temporal analysis, cluster sensitivity parameter: 40

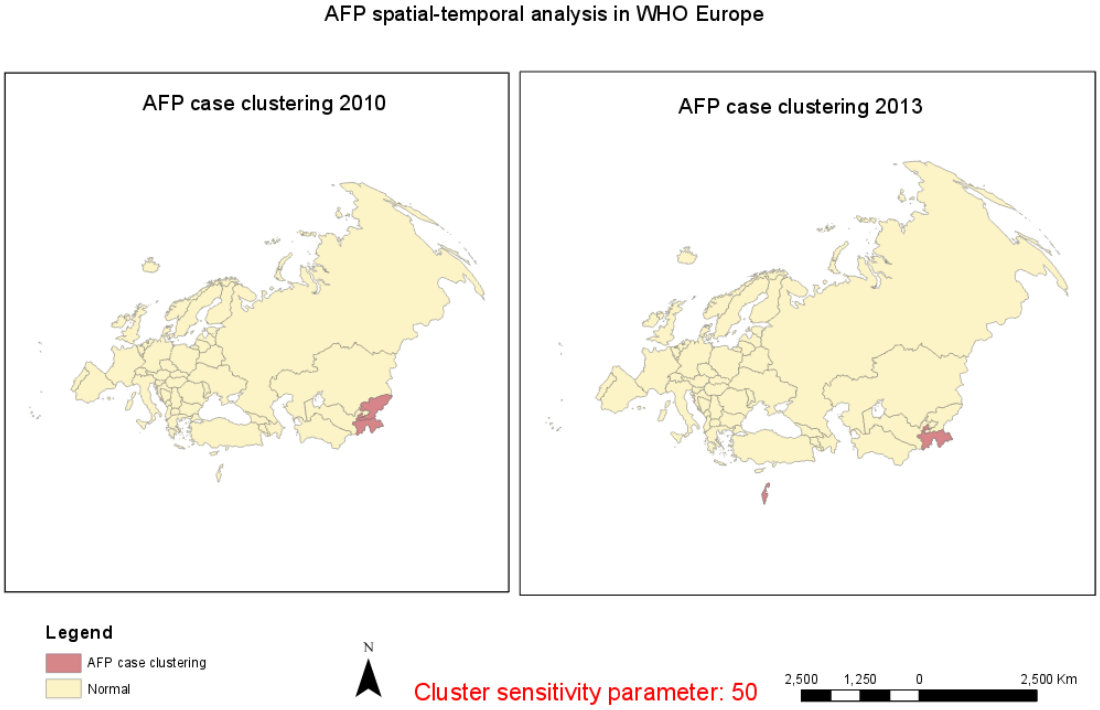

Figure 4-13: WHO Europe, spatial-temporal analysis, cluster sensitivity parameter: 50

4.2.2 Analysis of AFP cases, STCDL results

The analysis covered data for 2017-2018 which resulted in 12 steps; each year is one step. The STCDL requires a minimum of 10 steps. The resulting summary table was presented in Figure A-4. The Mann-Kendall trend statistics is not significant a with p-value of 0,3037 (higher then 95% confidence interval) and trend statistics of 1,0286.

Neighbors in space and time were used to fill the empty cubes, but still during the creation of the NetCDF structure 26 out of 54 defined locations were excluded from STCDL due to the presence of cubes that could not be estimated. A minimum of 4 neighbors are required to fill empty cubes using the average value of spatial neighbors, and a minimum of 13 neighbors are required to fill empty cubes using the average value of space time neighbors[19] .

The final map with hot spot cubes is shown in figure 4-14. Even though the trend is insignificant, the outbreak in the region was depicted by three countries Tajikistan, Kyrgyzstan and Russian Federation.

The STCDL analysis did show an issue in the Russian Federation. There was a spread of polio virus outbreak during 2010, but it was incorrect to show that it happened for such a long period. The overall trend is not significant and it was considered an error.

[19] "How Creating a Space Time Cube works"; page 20

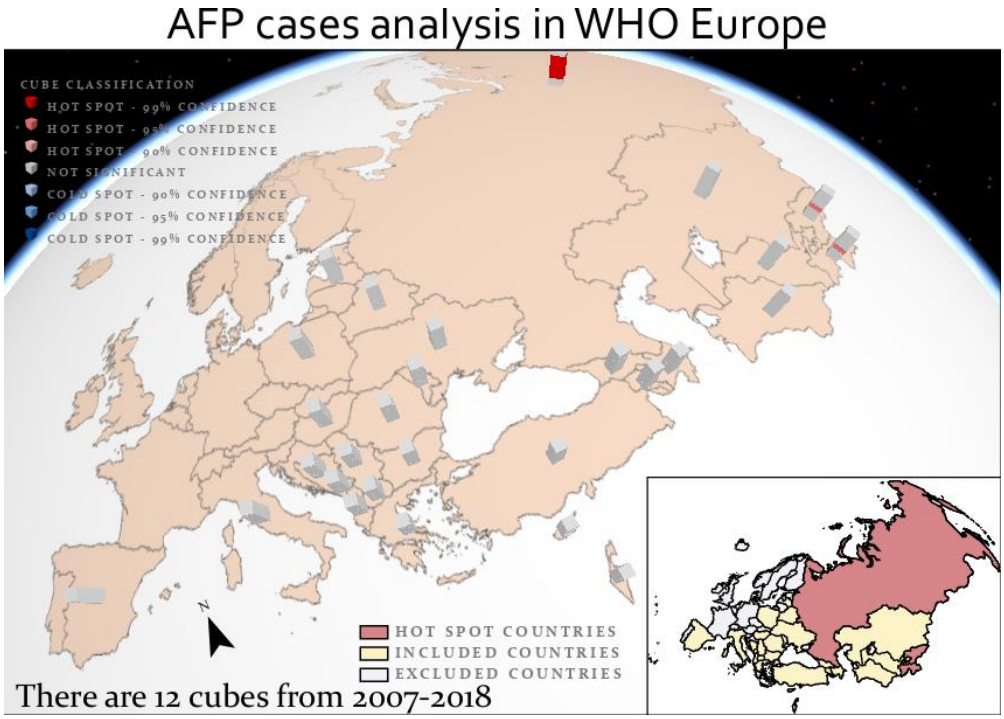

Figure 4-14: WHO Europe, AFP cases analysis using STCDL using sum for aggregation

4.2.3 Analysis of zero dose cases, SACD results

The result of the SACD analysis of the WHO European region for zero dose cases was presented in figure 4-15. A cluster parameter of five was used since the amount of AFP zero dose cases is significantly lower compared to the previous AFP cases analysis.

The map shows a significant clustering of AFP zero doses in Eastern part of Europe for all years. According to WHO/UNICEF estimates: Romania and Ukraine are countries with low polio (Pol3) vaccination coverage and considered high risk countries for polio outbreak (Khetsuriani et. al 2014).

Also, Israel had been shown with high clustering of AFP zero doses. According to WHO/UNICEF report it had low vaccination coverage in the past (Khetsuriani et. al 2014).

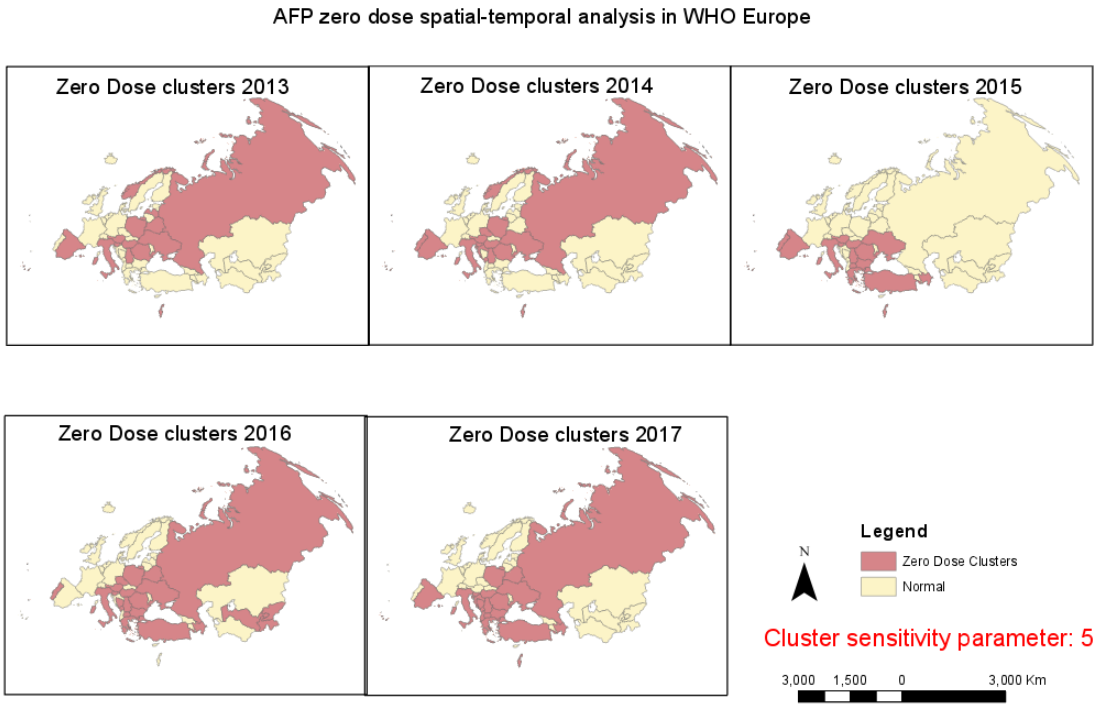

Figure 4-15: WHO Europe, AFP zero-dose cases analysis using SACD, cluster sensitivity parameter: 5

4.2.4 Analysis of zero dose cases, STCDL result

As in previous report STCDL report, the 12 year period was used to perform the analysis. The Mann-Kendall trend statistics is increasing and significant with a p-value of 0,0269 and a trend statistics of 2,2135. During the execution of the analysis 49 out of 54 defined locations were removed from the analysis due to cubes that could not be estimated. The STCDL summary table was presented in figure A-5.

The STCDL result was shown in figure 4-16. Although all remaining countries in the analysis possess insignificant cubes, still few countries did possess an interest. Ukraine, Romania and Israel were among the countries that were found with zero doses AFP clustering. As mentioned by Khetsuriani, these countries are among those with low polio vaccination coverage.

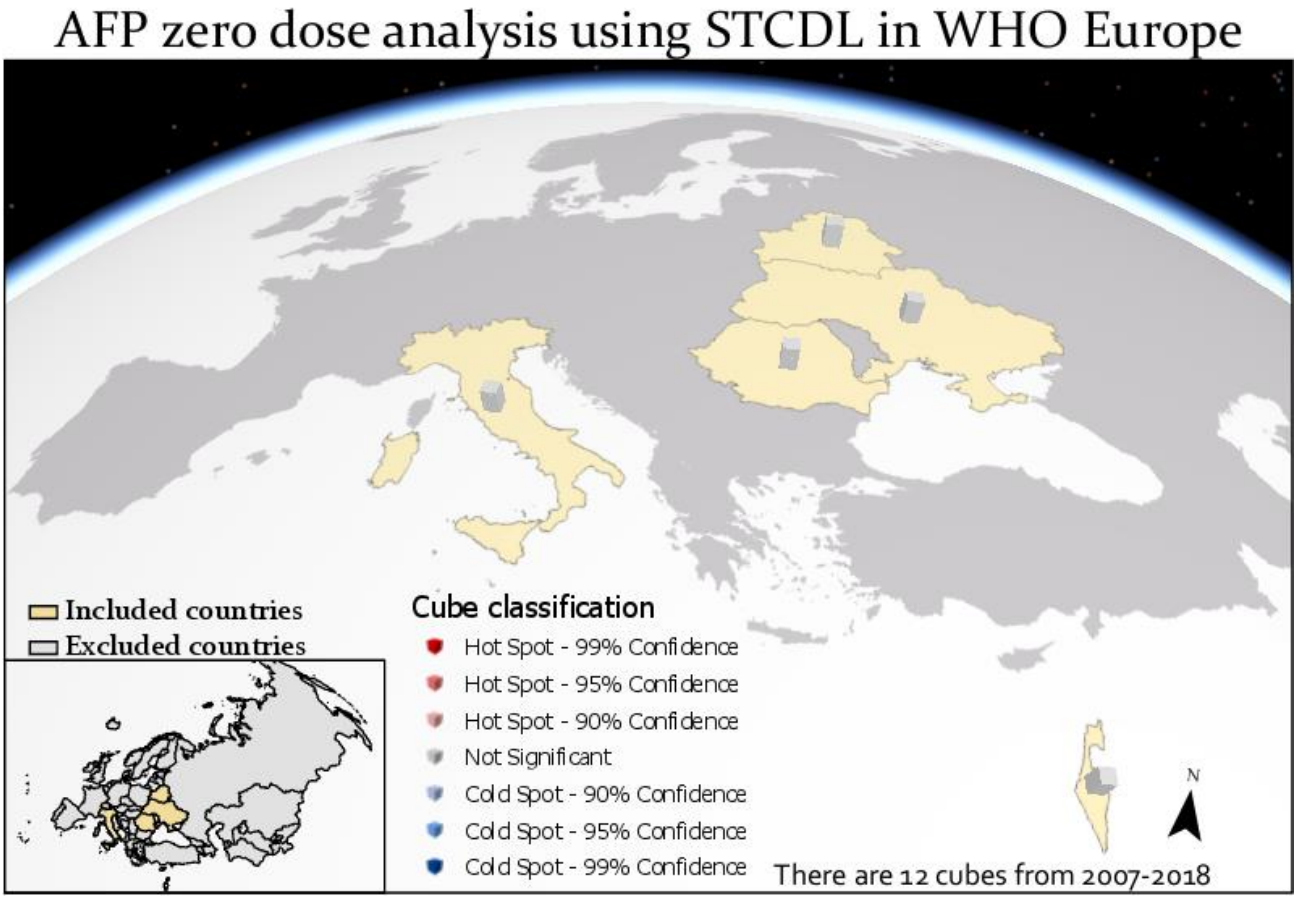

Figure 4-16: WHO Europe, AFP Zero cases analysis using STCDL, using sum for aggregation

5 DISCUSSION

5.1 Comparison between SACD and STCDL

This research has utilized two approaches to analyze previously reported information and has identified unusual clustering of diseases in space and time. First, an algorithm called SACD was developed specifically for this assignment to isolate those areas related to polio. Secondly, scientifically proven Mann-Kendall and Getis-Ord Gi methods, described in STCDL algorithm have been chosen to find patterns in two study areas: Nigeria and WHO Europe.

The SACD algorithm was controlled by a sensitivity cluster parameter, which was dependent on the amount of input data. For Nigeria with more than 64 000 AFP cases reported in the past five years, cluster parameters of 30 and 100 were used. For WHO Europe with more than 19 000 AFP cases reported within the past 12 years, it was used cluster parameters of 40 and 50. In addition, a fraction of reported cases were utilized in the analysis of circumstances involving of non-vaccinated (Zero doses) children. Kindly note, that monitoring these cases are important factors for polio eradication. For this situation where total AFP zero doses correspond to 926 cases in Nigeria a much lower cluster sensitivity parameter was used, respectively: 2, 3 and 5.

Although there was a correlation between the size the of data and cluster sensitivity, in SACD, there was no direct guidance on how the cluster sensitivity parameter was decided. Instead, a trial of many parameters were used to detect these clustered territories. In contrast, STCDL algorithm relied on statistical models, which provided scientifically proven results based on probabilistic statistical methods.

STCDL has a disadvantage that it requires a high amount of input. In addition, it needs at least ten times the number of period steps and each location must have a value at every time step. There must be a decision on how to complete the time series using the method of filling empty cubes with a value taken from their neighbors in space and time. The SACD algorithm does not require a complete time series, but it removes those locations that have empty values (No AFP cases were reported).

SACD and STCDL analyses were almost identical in nature because they were using similar input data and generated reports for the same defined geographical location. Also, the results yielded cluster in close semblance. For example, in Nigeria there was

an issue in the North-Eastern part of the country (Inwa Barau et. al 2014). Both algorithms have detected these outbreaks in zero dose cases analysis. There was a significant difference between results of these two algorithms in analysis of the total number of cases. STCDL showed a clear issue in Northern Nigeria (Figure 4-5) and the SACD were distributed across Nigeria.

Finally, the major multi-national outbreak of polio in 2010 in Tajikistan (Khetsuriani et. al 2014) and one in Israel 2013 (Khetsuriani et. al 2014) were detected and visualized by both SACD and STCDL.

To keep the STCDL analysis manageable it was decided to aggregate them with 37 provinces at the first administrative level. However, visualizing the cubes consumed a large portion of GPU and memory. Conducting the STCDL analysis using more than 100 locations would become very difficult for on one computer. To visualize 37 provinces, required removing hardware limits and waiting approximately five minutes. In contrast, the prototype used to collapse data at the district level, which consists of more than 700 locations for Nigeria and on same computer the results were generated in around two minutes. Thus, SACD is executed faster with the same computer resources.

Another difference between the analyses was how temporary aggregation has been performed. When creating an STCDL cube from defined locations with temporal aggregation a summary field statistics has to be chosen. There were several options for summary: sum, mean, min, max, standard deviation within the cube and median[20]. The goal was to find a significant difference in all territories (not only the minimum or maximum) and mean was utilized in the SACD algorithm from beginning, as well as in STCDL.

5.2 Integration of analyses into an outbreak prevention system

Finally a very important aspect of this research was to investigate how to automatize the process of creating the SACD and STCDL reports into a Standard Operational Procedure (SOP). The aim was to organize them into an outbreak prevention system that would cover many countries and territories. Each country has different

[20] "How Creating a Space Time Cube works", page 20

requirements and possibilities for data reporting. For example, in a situation of a disease outbreak an AFP case base surveillance would be insufficient, and an aggregate reporting system would be optimal to save time. The geographical information and time are very important for epidemiologists to investigate an outbreak.

At the regional level WHO Europe, (Vaccine-preventable Diseases and Immunization Programme of WHO Europe) VPI was using (Centralized Information System for Infectious Diseases) CISID and (Laboratory Data Management System) LDMS to collect AFP cases and laboratory sample data (Figure A-5). These systems have been provided to member states both aggregated (in case of outbreak) and case based reporting capabilities.

A key functionality designed by VPI and implemented in LDMS was “weekly AFP temporal clustering alerts”. It was a program that ran automatically on a weekly basis. The algorithm verified each country and when a reported AFP cases did exceed a threshold of cumulative cases reported in the past year then it would generate a table report with countries and the total number of hot cases (Figure A-5). In addition, it has implemented some restrictions for “hot” AFP cases.

Finally, the algorithm will detect if there are potential hot cases and then output would be sent by email to the focal point (epidemiologist). The analysis developed here could be integrated with cluster maps of cases and help with early warning.

The main issue addressed in this paper was to utilize the borders between existing countries to analyze reported AFP cases and generate reports for potential clustering. More specifically, the developed analysis could be integrated into an automatic SOP for the creation of routine reports and potential outreach, thus informing focal points of such unusual situations (Listing 4-1). SACD algorithm program was modularized so it could be easily integrated into the LDMS “hot” AFP case algorithm and routinely used by health specialists (Listing 4-1).

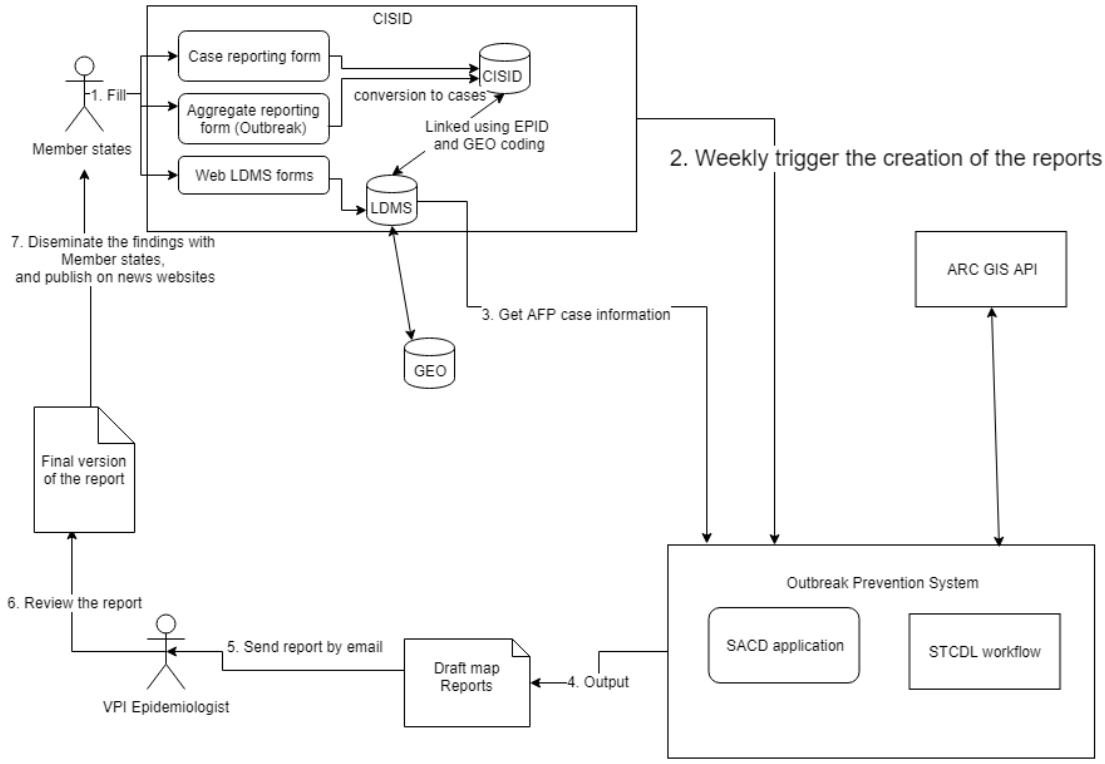

Listing 4-1: Outbreak prevention system data workflow

In summary, the health specialists from members states fill-in the forms with AFP cases (Listing 4-1 step 1) on a weekly basis in the CISID. Then a map report analysis is generated each week (Listing 4-1 step 2). When a report contains clusters of hot AFP cases, then it would be sent by email for a review to a VPI epidemiologist (Listing 4-1 step 4 and 5). He would be responsible for verifying the accuracy, creating the final version of the report and disseminating the results among member states, and publishing it on the website (Listing 4-1 step 6 and 7). Automatic reports like STCDL, and SACD should not be published directly, but their results should be verified and clarified before they are disseminated.

6 CONCLUSIONS

In order to fulfill the requirements for this paper an experimental prototype application has been developed that implemented SACD algorithm. Fortunately, during the data research it was found that Arc GIS Pro, which is a new product from ESRI, supports a similar method for analysis that meets the needs for this study. This was not possible to do in ArcMap, and therefore for this paper a license for ArcGIS Pro was offered by WHO. This made possible for this work to use both SACD prototype and STCDL implementation. These techniques were used to explore spatio-temporal clustering for two case studies: Nigeria and the WHO European region.

Furthermore, with regards to the first objective, this prototype (SACD algorithm) was designed to determine defined location with significant clustering of cases. Using the supplied dataset of AFP cases the analysis has been executed successfully.

In comparison to STCDL that relies on probabilistic determinants, the SACD does consider using of a sensitivity cluster parameter. Although there was a direct correlation between the input data and cluster sensitivity, still number of tests were carried out to determine the optimal parameter for cluster sensitivity. As a rule of thumb, a low parameter is tested first, then gradually increased until an optimal picture with defined location clusters was obtained. Both newly developed model SACD and validation model STCDL have demonstrated a significant clustering issue of AFP cases in the northen part of Nigeria.

One of the more significant findings to emerge from this study was from spatio-temporal analyses in WHO Europe. As of result a new innovative SACD the multi-national polio outbreak in 2010 (Khetsuriani et. al 2014) have been spotted. It started in Tajikistan and spread to neighboring countries. It was followed by a massive SIA vaccination for children and the polio outbreak stopped in the same year (Khetsuriani et. al 2014). Another major finding by SACD, was identified in Israel, another polio outbreak detected in 2013 in the WHO European region (Khetsuriani et. al 2014). Also, the validation model STCDL was in most part consistent with SACD.

The second objective, of this paper was to evaluate the vulnerable unvaccinated children. In this investigation, the aim was to assess AFP cases with zero dose vaccinations which is a small fraction of total AFP cases reported. As the input data

was considerably less than in previous analyses, the cluster sensitivity parameters were respectively lower. Nevertheless, the SACD and STCDL have identified an issue in the North-East of Nigeria. In addition, the South-East part of Europe identified a significant cluster. Romania and Ukraine were considered particularly high risk countries because of low polio vaccination coverage (Khetsuriani et. al 2014).

The evidence from this study suggests that there is no active outbreak in WHO Europe in the past year, but there were still major issues in Nigeria. These analyses could have a practical application in routinely usage, if incorporated in an outbreak prevention system. It would analyze the reported data on a defined time period (for example weekly). If something unusual was detected then health specialists would be informed so they could take further prevention actions.

References

Abatan A. Abayomi, Babatunde J. Abiodun, William J. Gutowski, Saidat O. Rasaq-Balogun; *Trends and variability in absolute indices of temperature extremes over Nigeria: linkage with NAO*; 2017; Royal Meteorological Society; International Journal of Climatology; vol 38; no. 2; pp. 593-612

Elliott Paul and Daniel Wartenberg; *Spatial Epidemiology: Current Approaches and Future Challenges*; 2004; Environmental Health Perspective; vol. 112; no.9; pp. 998–1006

Ibrahim Sa'ad,Isah Hamisu, Usman Lawal; *Spatial Pattern of Tuberculosis Prevalence in Nigeria: A Comparative Analysis of Spatial Autocorrelation Indices*; 2015; American Journal of Geographic Information System; vol. 2; no. 3; pp 87-94

Khetsuriani Nino, Dina Pfeifer, Sergei Deshevoi, Eugene Gavrilin, Abigail Shefer, Robb Butler, Dragan Jankovic, Roman Spataru, Nedret Emiroglu, and Rebecca Martin. *Challenges of Maintaining Polio-free Status of the European Region*; 2014; The Journal of Infectious Disease; Oxford University Press; vol. 210; no. 1; pp. S194-S207;

Mahara Gehendra, Chao Wang, Da Huo, Qin Xu, Fangfang Huang, Lixin Tao, Jin Guo, Kai Cao, Liu Long, Jagadish K. Chhetri, Qi Gao, Wei Wang, Quanyi Wang and Xiuhua Guo; *Spatiotemporal Pattern Analysis of Scarlet Fever Incidence in Beijing, China, 2005–2014*; 2016; International Journal Environmental Research and Public Health; vol. 13; no. 131; pp. 2-17

Rogerson Peter A.; *Statistical Methods for Geography*; 2015; Fourth Edition; SAGE Publications; ISBN 9780761962878;

Tango Toshiro; *Statistical Methods for Disease Clustering*; 2010; Springer New York, ISBN: 9781441915726;

Tlou Boikhutso, Benn Sartorius1, Frank Tanser1*; Space-time variations in child mortality in a rural South African population with high HIV prevalence (2000–2014)*; 2017; A Peer-Reviewed Open Access Journal (PLoS One); vol. 12; no. 8; pp. 1-13

Toshiro Tango, Kunihiko Takahashi; *A flexibly shaped spatial scan statistic for detecting clusters*; 2005; 10.1186/1476-072X-4-11; International Journal of Health Geographics; vol. 4; no. 1; pp. 1-15

Uittenbogaard Adriaan and Vania Ceccato*; Space-time Clusters of Crime in Stockholm*, Sweden; 2012; Review of European Studies; Published by Canadian Center of Science and Education; vol. 4; no. 5; pp. 148-156

Zhao Fei, Shiming Cheng1, Guangxue He1, Fei Huang1, Hui Zhang1, Biao Xu, Tonderayi C. Murimwa, Jun Cheng1, Dongmei Hu1, Lixia Wang1; *Space-Time Clustering Characteristics of Tuberculosis in China, 2005-2011*; 2013; A Peer-Reviewed Open Access Journal (PLoS One); vol. 8; no. 12; pp. 1-7

Appendix A

```
Running script CreateSpaceTimeCubeDefinedLocations...
---------- Space Time Cube Characteristics -----------
Input feature time extent          2013-01-01 00:00:00
                                 to 2017-10-01 00:00:00

Number of time steps                                 10
Time step interval                            6 months
Time step alignment                                End

First time step temporal bias                    50,55%
First time step interval                          after
                                  2012-10-01 00:00:00
                                      to on or before
                                  2013-04-01 00:00:00

Last time step temporal bias                      0,00%
Last time step interval                           after
                                  2017-04-01 00:00:00
                                      to on or before
                                  2017-10-01 00:00:00

Cube extent across space       (coordinates in meters)
Min X                                          2,6925
Min Y                                          4,2725
Max X                                         14,6581
Max Y                                         13,8915

Locations                                          37
% of locations with estimated observations       0,00
- Total number                                      0
Total observations                                370
% of all observations that were estimated         0,00
- Total number                                      0

- Overall Data Trend - NRC_MEAN_SPACE_TIME_NEIGHBORS -
Trend direction                             Increasing
Trend statistic                                 2,8622
Trend p-value                                   0,0042

-- Overall Data Trend - TEMPORAL_AGGREGATION_COUNT ---
Trend direction                         Not Significant
Trend statistic                                -0,1113
Trend p-value                                   0,9113
Completed script Create Space Time Cube From Defined Locations...
```

Figure A-1:Nigeria, AFP cases, space-time cube summary, using MEAN for aggregation

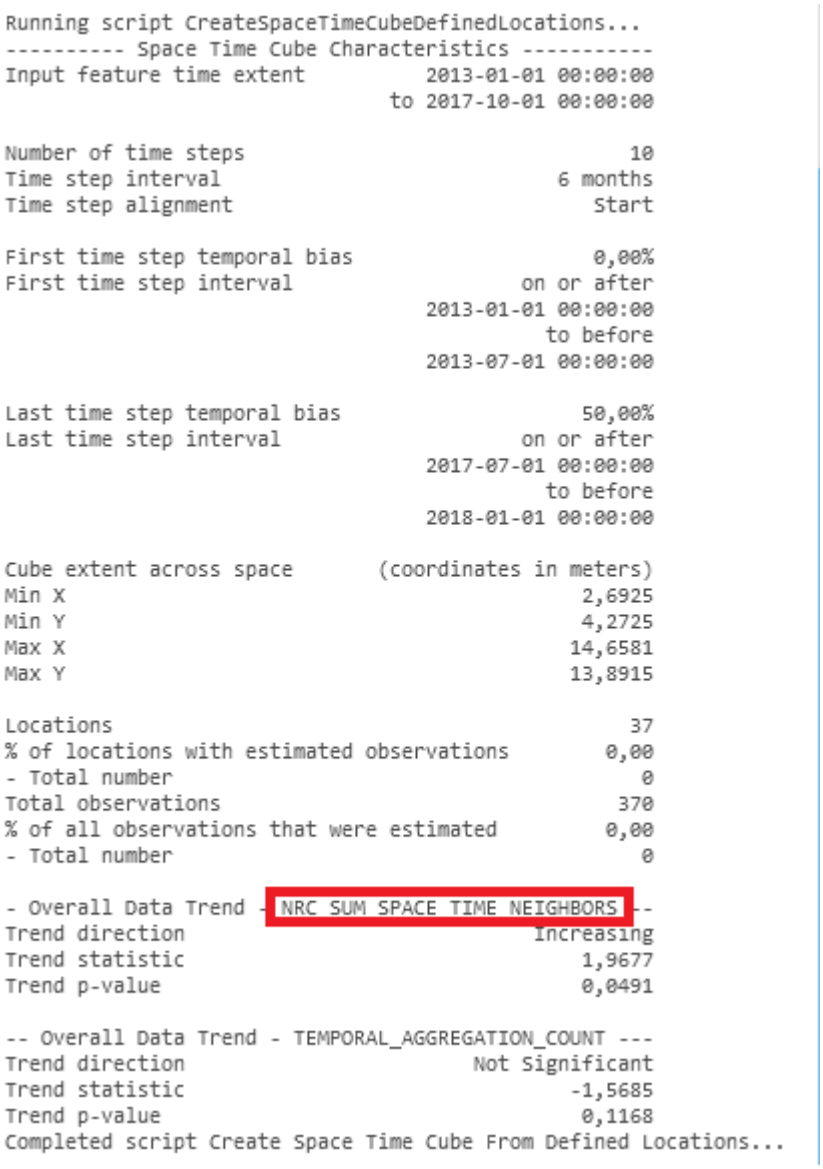

```
Running script CreateSpaceTimeCubeDefinedLocations...
---------- Space Time Cube Characteristics -----------
Input feature time extent          2013-01-01 00:00:00
                                to 2017-10-01 00:00:00

Number of time steps                                 10
Time step interval                            6 months
Time step alignment                              Start

First time step temporal bias                     0,00%
First time step interval                   on or after
                                  2013-01-01 00:00:00
                                            to before
                                  2013-07-01 00:00:00

Last time step temporal bias                     50,00%
Last time step interval                    on or after
                                  2017-07-01 00:00:00
                                            to before
                                  2018-01-01 00:00:00

Cube extent across space       (coordinates in meters)
Min X                                          2,6925
Min Y                                          4,2725
Max X                                         14,6581
Max Y                                         13,8915

Locations                                          37
% of locations with estimated observations       0,00
- Total number                                      0
Total observations                               370
% of all observations that were estimated        0,00
- Total number                                      0

- Overall Data Trend - NRC_SUM_SPACE_TIME_NEIGHBORS --
Trend direction                             Increasing
Trend statistic                                1,9677
Trend p-value                                  0,0491

-- Overall Data Trend - TEMPORAL_AGGREGATION_COUNT ---
Trend direction                         Not Significant
Trend statistic                                -1,5685
Trend p-value                                  0,1168
Completed script Create Space Time Cube From Defined Locations...
```

Figure A-2: Nigeria, AFP cases, space-time cube summary, using SUM for aggregation

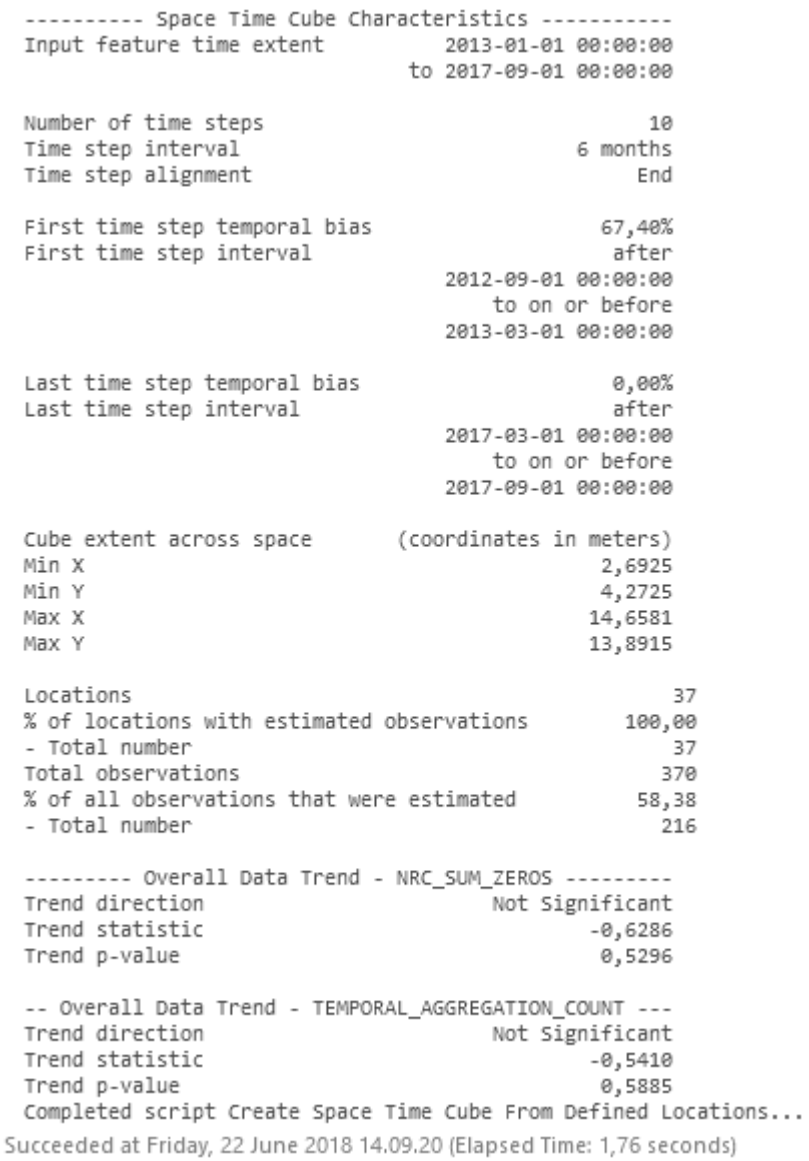

Figure A-3: Nigeria, zero dose AFP cases, space-time cube summary, using SUM for aggregation

```
Running script CreateSpaceTimeCubeDefinedLocations...
⚠ WARNING 110089: 26 out of 54 Defined Locations were excluded
from the Space Time Cube due to the presence of bins that could not
be estimated.
⚠ WARNING 110090: Defined Locations excluded from the Space Time
Cube based on the inability to predict (only includes first 30):
OBJECTID3 = 5, 13, 20, 198, 54, 79, 58, 67, 72, 73, 216, 51, 100,
95, 2747, 118, 119, 133, 125, 142, 152, 164, 197, 187, 186, 179.
---------- Space Time Cube Characteristics -----------
Input feature time extent          2007-01-01 00:00:00
                                 to 2018-03-01 00:00:00

Number of time steps                                 12
Time step interval                              1 year
Time step alignment                              Start

First time step temporal bias                     0,00%
First time step interval                   on or after
                                  2007-01-01 00:00:00
                                             to before
                                  2008-01-01 00:00:00

Last time step temporal bias                     83,84%
Last time step interval                    on or after
                                  2018-01-01 00:00:00
                                             to before
                                  2019-01-01 00:00:00

Cube extent across space       (coordinates in meters)
Min X                                   -5032875,9013
Min Y                                    -562310,0299
Max X                                    4699990,4197
Max Y                                    5823167,2019

Locations                                           28
% of locations with estimated observations       21,43
- Total number                                      6
Total observations                                336
% of all observations that were estimated         2,98
- Total number                                     10

- Overall Data Trend - NRC_SUM_SPACE_TIME_NEIGHBORS --
Trend direction                         Not Significant
Trend statistic                                1,0286
Trend p-value                                  0,3037

-- Overall Data Trend - TEMPORAL_AGGREGATION_COUNT ---
Trend direction                         Not Significant
Trend statistic                               -0,7702
Trend p-value                                  0,4412
Completed script Create Space Time Cube From Defined Locations...
```

Figure A-4: WHO Europe, AFP cases, space-time cube summary, using SUM for aggregation

```
Running script CreateSpaceTimeCubeDefinedLocations...
⚠ WARNING 110089: 49 out of 54 Defined Locations were excluded
from the Space Time Cube due to the presence of bins that could not
be estimated.
⚠ WARNING 110090: Defined Locations excluded from the Space Time
Cube based on the inability to predict (only includes first 30):
OBJECTID3 = 5, 2, 10, 13, 14, 26, 20, 31, 198, 228, 53, 54, 79, 58,
67, 191, 72, 73, 216, 78, 82, 51, 94, 100, 95, 110, 106, 2747, 118,
119.
---------- Space Time Cube Characteristics -----------
Input feature time extent          2007-01-01 00:00:00
                                to 2018-03-01 00:00:00

Number of time steps                                12
Time step interval                           1 year
Time step alignment                           Start

First time step temporal bias                    0,00%
First time step interval                 on or after
                                    2007-01-01 00:00:00
                                              to before
                                    2008-01-01 00:00:00

Last time step temporal bias                    83,84%
Last time step interval                  on or after
                                    2018-01-01 00:00:00
                                              to before
                                    2019-01-01 00:00:00

Cube extent across space       (coordinates in meters)
Min X                                   -2958291,1842
Min Y                                    -562310,0299
Max X                                    -346681,0199
Max Y                                    2387704,0379

Locations                                           5
% of locations with estimated observations      60,00
- Total number                                     3
Total observations                                60
% of all observations that were estimated       8,33
- Total number                                     5

- Overall Data Trend - NRC_SUM_SPACE_TIME_NEIGHBORS --
Trend direction                           Increasing
Trend statistic                              2,2135
Trend p-value                                0,0269

-- Overall Data Trend - TEMPORAL_AGGREGATION_COUNT ---
Trend direction                       Not Significant
Trend statistic                              1,4468
Trend p-value                                0,1479
Completed script Create Space Time Cube From Defined Locations...
```

Figure A-5: WHO Europe, zero dose AFP cases, space-time cube summary, using SUM for aggregation

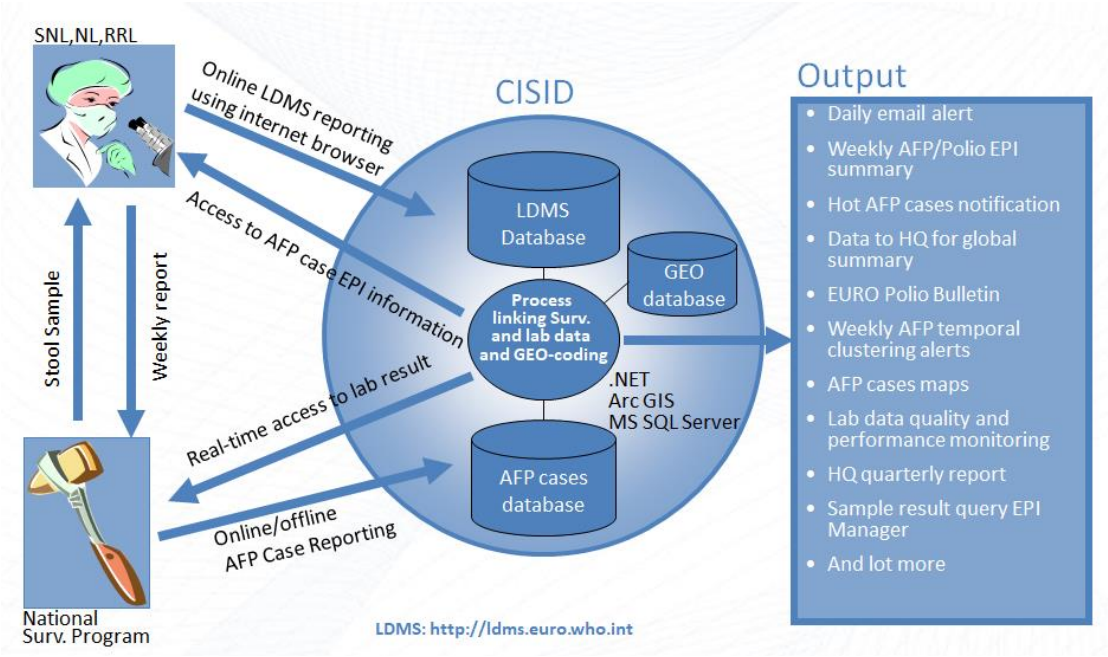

Figure A-6: Online LDMS and CISID workflow

Appendix B

ESRI, Environmental Systems Research Institute; *An overview of the Spatial Statistics toolbox*; [Online] Available at: http://pro.arcgis.com/en/pro-app/tool-reference/spatial-statistics/an-overview-of-the-spatial-statistics-toolbox.htm [Accessed 17 March 2018]

ESRI; *How Creating a Space Time Cube works*; [Online] Available at: http://pro.arcgis.com/en/pro-app/tool-reference/space-time-pattern-mining/learnmorecreatecube.htm [Accessed 17 March 2018]

ESRI; *How Emerging Hot Spot analysis work*; [Online] Available at: http://desktop.arcgis.com/en/arcmap/10.3/tools/space-time-pattern-mining-toolbox/learnmoreemerging.htm [Accessed 17 March 2018]

ESRI; *How Hot Spot Analysis (Getis-Ord Gi) works*; [Online] Available at: http://pro.arcgis.com/en/pro-app/tool-reference/spatial-statistics/h-how-hot-spot-analysis-getis-ord-gi-spatial-stati.htm [Accessed 17 March 2018]

ESRI; *Spatial Statistics*; [Online] Available at: https://spatialstats.github.io/presentations/ [Accessed 17 March 2018]

Khambhammettu Prashanth; *Mann-Kendall statistics memorandum*; 2005; Annual Groundwater Monitoring Report; [Online] Available at: http://www.statisticshowto.com/wp-content/uploads/2016/08/Mann-Kendall-Analysis-1.pdf [Accessed 17 March 2018]

Lixin Huang; *Analyzing traffic accidents in space and time*; [Online] Available at: http://desktop.arcgis.com/en/analytics/case-studies/analyzing-crashes-1-overview.htm [Accessed 17 March 2018]

Unidata's Network Common Data Form; *NetCDF Fact Sheet*; [Online] Available at: https://www.unidata.ucar.edu/publications/factsheets/current/factsheet_netcdf.pdf [Accessed 17 March 2018]

WHO European Region; *Report of the 30th Meeting of the European RCC for Poliomyelitis Eradication*; 2016; [Online] Available at: http://www.euro.who.int/en/health-topics/communicable-diseases/poliomyelitis/publications/2016/30th-meeting-of-the-european-

regional-certification-commission-for-poliomyelitis-eradication [Accessed 17 March 2018]

WHO; *Factsheet Polio Euro*; [Online] Available at: http://www.euro.who.int/__data/assets/pdf_file/0005/276485/Factsheet-Polio-en.pdf [Accessed 17 March 2018]

WHO; *Poliomyelitis, key facts*; [Online] Available at: http://www.who.int/news-room/fact-sheets/detail/poliomyelitis [Accessed 17 March 2018]

WHO; *WHO Removes Nigeria from Polio-Endemic List*; [Online] Available at: http://www.who.int/mediacentre/news/releases/2015/nigeria-polio/en/ [Accessed 17 March 2018]

Series from Lund University

Department of Physical Geography and Ecosystem Science

Master Thesis in Geographical Information Science

1. *Anthony Lawther:* The application of GIS-based binary logistic regression for slope failure susceptibility mapping in the Western Grampian Mountains, Scotland (2008).
2. *Rickard Hansen:* Daily mobility in Grenoble Metropolitan Region, France. Applied GIS methods in time geographical research (2008).
3. *Emil Bayramov:* Environmental monitoring of bio-restoration activities using GIS and Remote Sensing (2009).
4. *Rafael Villarreal Pacheco:* Applications of Geographic Information Systems as an analytical and visualization tool for mass real estate valuation: a case study of Fontibon District, Bogota, Columbia (2009).
5. *Siri Oestreich Waage:* a case study of route solving for oversized transport: The use of GIS functionalities in transport of transformers, as part of maintaining a reliable power infrastructure (2010).
6. *Edgar Pimiento:* Shallow landslide susceptibility – Modelling and validation (2010).
7. *Martina Schäfer:* Near real-time mapping of floodwater mosquito breeding sites using aerial photographs (2010).
8. *August Pieter van Waarden-Nagel:* Land use evaluation to assess the outcome of the programme of rehabilitation measures for the river Rhine in the Netherlands (2010).
9. *Samira Muhammad:* Development and implementation of air quality data mart for Ontario, Canada: A case study of air quality in Ontario using OLAP tool. (2010).
10. *Fredros Oketch Okumu*: Using remotely sensed data to explore spatial and temporal relationships between photosynthetic productivity of vegetation and malaria transmission intensities in selected parts of Africa (2011).
11. *Svajunas Plunge:* Advanced decision support methods for solving diffuse water pollution problems (2011).
12. *Jonathan Higgins:* Monitoring urban growth in greater Lagos: A case study using GIS to monitor the urban growth of Lagos 1990 - 2008 and produce future growth prospects for the city (2011).
13. *Mårten Karlberg:* Mobile Map Client API: Design and Implementation for Android (2011).
14. *Jeanette McBride:* Mapping Chicago area urban tree canopy using color infrared imagery (2011).
15. *Andrew Farina:* Exploring the relationship between land surface temperature and vegetation abundance for urban heat island mitigation in Seville, Spain (2011).
16. *David Kanyari*: Nairobi City Journey Planner: An online and a Mobile Application (2011).

17. *Laura V. Drews:* Multi-criteria GIS analysis for siting of small wind power plants - A case study from Berlin (2012).
18. *Qaisar Nadeem:* Best living neighborhood in the city - A GIS based multi criteria evaluation of ArRiyadh City (2012).
19. *Ahmed Mohamed El Saeid Mustafa:* Development of a photo voltaic building rooftop integration analysis tool for GIS for Dokki District, Cairo, Egypt (2012).
20. *Daniel Patrick Taylor*: Eastern Oyster Aquaculture: Estuarine Remediation via Site Suitability and Spatially Explicit Carrying Capacity Modeling in Virginia's Chesapeake Bay (2013).
21. *Angeleta Oveta Wilson:* A Participatory GIS approach to *unearthing* Manchester's Cultural Heritage '*gold mine'* (2013).
22. *Ola Svensson:* Visibility and Tholos Tombs in the Messenian Landscape: A Comparative Case Study of the Pylian Hinterlands and the Soulima Valley (2013).
23. *Monika Ogden:* Land use impact on water quality in two river systems in South Africa (2013).
24. *Stefan Rova:* A GIS based approach assessing phosphorus load impact on Lake Flaten in Salem, Sweden (2013).
25. *Yann Buhot:* Analysis of the history of landscape changes over a period of 200 years. How can we predict past landscape pattern scenario and the impact on habitat diversity? (2013).
26. *Christina Fotiou:* Evaluating habitat suitability and spectral heterogeneity models to predict weed species presence (2014).
27. *Inese Linuza:* Accuracy Assessment in Glacier Change Analysis (2014).
28. *Agnieszka Griffin:* Domestic energy consumption and social living standards: a GIS analysis within the Greater London Authority area (2014).
29. *Brynja Guðmundsdóttir:* Detection of potential arable land with remote sensing and GIS - A Case Study for Kjósarhreppur (2014).
30. *Oleksandr Nekrasov:* Processing of MODIS Vegetation Indices for analysis of agricultural droughts in the southern Ukraine between the years 2000-2012 (2014).
31. *Sarah Tressel:* Recommendations for a polar Earth science portal in the context of Arctic Spatial Data Infrastructure (2014).
32. *Caroline Gevaert:* Combining Hyperspectral UAV and Multispectral Formosat-2 Imagery for Precision Agriculture Applications (2014).
33. *Salem Jamal-Uddeen:* Using GeoTools to implement the multi-criteria evaluation analysis - weighted linear combination model (2014).
34. *Samanah Seyedi-Shandiz:* Schematic representation of geographical railway network at the Swedish Transport Administration (2014).
35. *Kazi Masel Ullah:* Urban Land-use planning using Geographical Information System and analytical hierarchy process: case study Dhaka City (2014).
36. *Alexia Chang-Wailing Spitteler:* Development of a web application based on MCDA and GIS for the decision support of river and floodplain rehabilitation projects (2014).
37. *Alessandro De Martino:* Geographic accessibility analysis and evaluation of potential changes to the public transportation system in the City of Milan (2014).
38. *Alireza Mollasalehi:* GIS Based Modelling for Fuel Reduction Using Controlled Burn in Australia. Case Study: Logan City, QLD (2015).

39. *Negin A. Sanati:* Chronic Kidney Disease Mortality in Costa Rica; Geographical Distribution, Spatial Analysis and Non-traditional Risk Factors (2015).
40. *Karen McIntyre:* Benthic mapping of the Bluefields Bay fish sanctuary, Jamaica (2015).
41. *Kees van Duijvendijk:* Feasibility of a low-cost weather sensor network for agricultural purposes: A preliminary assessment (2015).
42. *Sebastian Andersson Hylander:* Evaluation of cultural ecosystem services using GIS (2015).
43. *Deborah Bowyer:* Measuring Urban Growth, Urban Form and Accessibility as Indicators of Urban Sprawl in Hamilton, New Zealand (2015).
44. *Stefan Arvidsson:* Relationship between tree species composition and phenology extracted from satellite data in Swedish forests (2015).
45. *Damián Giménez Cruz*: GIS-based optimal localisation of beekeeping in rural Kenya (2016).
46. *Alejandra Narváez Vallejo:* Can the introduction of the topographic indices in LPJ-GUESS improve the spatial representation of environmental variables? (2016).
47. *Anna Lundgren:* Development of a method for mapping the highest coastline in Sweden using breaklines extracted from high resolution digital elevation models (2016).
48. *Oluwatomi Esther Adejoro:* Does location also matter? A spatial analysis of social achievements of young South Australians (2016).
49. *Hristo Dobrev Tomov:* Automated temporal NDVI analysis over the Middle East for the period 1982 - 2010 (2016).
50. *Vincent Muller:* Impact of Security Context on Mobile Clinic Activities A GIS Multi Criteria Evaluation based on an MSF Humanitarian Mission in Cameroon (2016).
51. *Gezahagn Negash Seboka:* Spatial Assessment of NDVI as an Indicator of Desertification in Ethiopia using Remote Sensing and GIS (2016).
52. *Holly Buhler:* Evaluation of Interfacility Medical Transport Journey Times in Southeastern British Columbia. (2016).
53. *Lars Ole Grottenberg*: Assessing the ability to share spatial data between emergency management organisations in the High North (2016).
54. *Sean Grant:* The Right Tree in the Right Place: Using GIS to Maximize the Net Benefits from Urban Forests (2016).
55. *Irshad Jamal:* Multi-Criteria GIS Analysis for School Site Selection in Gorno-Badakhshan Autonomous Oblast, Tajikistan (2016).
56. *Fulgencio Sanmartín:* Wisdom-volkano: A novel tool based on open GIS and time-series visualization to analyse and share volcanic data (2016).
57. *Nezha Acil:* Remote sensing-based monitoring of snow cover dynamics and its influence on vegetation growth in the Middle Atlas Mountains (2016).
58. *Julia Hjalmarsson:* A Weighty Issue: Estimation of Fire Size with Geographically Weighted Logistic Regression (2016).
59. *Mathewos Tamiru Amato:* Using multi-criteria evaluation and GIS for chronic food and nutrition insecurity indicators analysis in Ethiopia (2016).
60. *Karim Alaa El Din Mohamed Soliman El Attar:* Bicycling Suitability in Downtown, Cairo, Egypt (2016).

61. *Gilbert Akol Echelai:* Asset Management: Integrating GIS as a Decision Support Tool in Meter Management in National Water and Sewerage Corporation (2016).
62. *Terje Slinning:* Analytic comparison of multibeam echo soundings (2016).
63. *Gréta Hlín Sveinsdóttir:* GIS-based MCDA for decision support: A framework for wind farm siting in Iceland (2017).
64. *Jonas Sjögren:* Consequences of a flood in Kristianstad, Sweden: A GIS-based analysis of impacts on important societal functions (2017).
65. *Nadine Raska:* 3D geologic subsurface modelling within the Mackenzie Plain, Northwest Territories, Canada (2017).
66. *Panagiotis Symeonidis*: Study of spatial and temporal variation of atmospheric optical parameters and their relation with PM 2.5 concentration over Europe using GIS technologies (2017).
67. *Michaela Bobeck:* A GIS-based Multi-Criteria Decision Analysis of Wind Farm Site Suitability in New South Wales, Australia, from a Sustainable Development Perspective (2017).
68. *Raghdaa Eissa*: Developing a GIS Model for the Assessment of Outdoor Recreational Facilities in New Cities Case Study: Tenth of Ramadan City, Egypt (2017).
69. *Zahra Khais Shahid*: Biofuel plantations and isoprene emissions in Svea and Götaland (2017).
70. *Mirza Amir Liaquat Baig*: Using geographical information systems in epidemiology: Mapping and analyzing occurrence of diarrhea in urban - residential area of Islamabad, Pakistan (2017).
71. *Joakim Jörwall*: Quantitative model of Present and Future well-being in the EU-28: A spatial Multi-Criteria Evaluation of socioeconomic and climatic comfort factors (2017).
72. *Elin Haettner*: Energy Poverty in the Dublin Region: Modelling Geographies of Risk (2017).
73. *Harry Eriksson*: Geochemistry of stream plants and its statistical relations to soil- and bedrock geology, slope directions and till geochemistry. A GIS-analysis of small catchments in northern Sweden (2017).
74. *Daniel Gardevärn:* PPGIS and Public meetings – An evaluation of public participation methods for urban planning (2017).
75. *Kim Friberg:* Sensitivity Analysis and Calibration of Multi Energy Balance Land Surface Model Parameters (2017).
76. *Viktor Svanerud:* Taking the bus to the park? A study of accessibility to green areas in Gothenburg through different modes of transport (2017).
77. *Lisa-Gaye Greene*: Deadly Designs: The Impact of Road Design on Road Crash Patterns along Jamaica's North Coast Highway (2017).
78. *Katarina Jemec Parker*: Spatial and temporal analysis of fecal indicator bacteria concentrations in beach water in San Diego, California (2017).
79. *Angela Kabiru*: An Exploratory Study of Middle Stone Age and Later Stone Age Site Locations in Kenya's Central Rift Valley Using Landscape Analysis: A GIS Approach (2017).
80. *Kristean Björkmann*: Subjective Well-Being and Environment: A GIS-Based Analysis (2018).
81. *Williams Erhunmonmen Ojo*: Measuring spatial accessibility to healthcare for people living with HIV-AIDS in southern Nigeria (2018).

82. *Daniel Assefa*: Developing Data Extraction and Dynamic Data Visualization (Styling) Modules for Web GIS Risk Assessment System (WGRAS). (2018).
83. *Adela Nistora*: Inundation scenarios in a changing climate: assessing potential impacts of sea-level rise on the coast of South-East England (2018).
84. *Marc Seliger*: Thirsty landscapes - Investigating growing irrigation water consumption and potential conservation measures within Utah's largest master-planned community: Daybreak (2018).
85. *Luka Jovičić*: Spatial Data Harmonisation in Regional Context in Accordance with INSPIRE Implementing Rules (2018).
86. *Christina Kourdounouli*: Analysis of Urban Ecosystem Condition Indicators for the Large Urban Zones and City Cores in EU (2018).
87. *Jeremy Azzopardi*: Effect of distance measures and feature representations on distance-based accessibility measures (2018).
88. *Patrick Kabatha*: An open source web GIS tool for analysis and visualization of elephant GPS telemetry data, alongside environmental and anthropogenic variables (2018).
89. *Richard Alphonce Giliba*: Effects of Climate Change on Potential Geographical Distribution of Prunus africana (African cherry) in the Eastern Arc Mountain Forests of Tanzania (2018).
90. *Eiður Kristinn Eiðsson*: Transformation and linking of authoritative multi-scale geodata for the Semantic Web: A case study of Swedish national building data sets (2018).
91. *Niamh Harty*: HOP!: a PGIS and citizen science approach to monitoring the condition of upland paths (2018).
92. *José Estuardo Jara Alvear*: Solar photovoltaic potential to complement hydropower in Ecuador: A GIS-based framework of analysis (2018).
93. *Brendan O'Neill*: Multicriteria Site Suitability for Algal Biofuel Production Facilities (2018).
94. *Roman Spataru*: Spatial-temporal GIS analysis in public health – a case study of polio disease (2018).